Japan Geoscience Union Meeting 2014
(28 April - 02 May 2014 at Pacifico YOKOHAMA, Kanagawa, Japan)

PPS21-01 Room:416 Time:April 29 09:00-09:15

The solidification of a magma ocean of Vesta

KAWABATA, Yusuke[1*] ; NAGAHARA, Hiroko[1]

[1]Earth and Planetary Science, The University of Tokyo

Asteroid 4 Vesta is the only preserved intact example of a large, differentiated protoplanet. Observations of surface spectra of Vesta provide convincing evidence for a differentiated interior. Vesta is considered as the parent body of HED meteorites.

Whether growing mineral grains remain suspended in the magma ocean or settled out is crucial for the primary interior structure of a planet.

The purpose of this study is to understand the role of grain size of crystals on solidification of a magma ocean under a turbulent flow. We select asteroid 4 Vesta as a subject of this study due to the presence of HED chondrites as a reference. In this study, we consider the solidification before the rheological transition occurs.

We assume that the interior structure of Vesta had already differentiated to form a core. We use the bulk silicate Vesta composition proposed by Righter and Drake (1998), which is a mixture of L and CV chondrites with the ratio of 7 to 3 adjusted for core separation. We calculate liquidus, solidus and solid fractions using the MELTs program (Ghiorso and Sack 1995; Asimow and Ghiorso 1998).In vigorously convective systems such as magma oceans, the temperature distribution is nearly adiabatic and isentropic (Solomatov, 2000).

The heat flux can be calculated with the help of the blackbody radiation. This heat flux must match the heat flux transported to the surface by convection. Convection changes to a regime sometimes called hard turbulence at very high Rayleigh number such as those in the magma ocean, of which heat flux is shown by Siggia (1994).

To describe the rate at which particles settle out of a turbulently convective fluid, we use the model by Martin & Nokes (1989).The particle number is calculated by

$dN/dt=N(-g\triangle\rho a^2)/(18\rho\nu h)$

where N is the particle number, g is the acceleration due to gravity, a is the diameter of the particle, $\triangle\rho$ is the density difference between the crystal and the magma, ν is the kinematic viscosity, and h is the depth of the fluid layer (Martin & Nokes, 1989).

The adiabat, liquidus and solidus of the magma ocean of Vesta are very steep, that is, they have negligibly small dependence on pressure.

Thermodynamic calculations with the MELTs program showed that olivine is the first liquidus phase at ˜1900K, followed by orthopyroxene and spinel. At the very late stage, clinopyroxene appears consuming orthopyroxene if chemical equilibrium is maintained.

The fluid dynamic evaluation shows that a very small fraction of crystals are separated from the magma ocean until the rheological transition which varied from 100um to 1cm in the current work. The thickness increases with time, which is shown in Figure.

Evaluation of fluid dynamic regime shows that the magma ocean on Vesta was at the hard turbulence regime, suggesting near equilibrium crystallization until the rheological transition takes place at the crystal fraction of 60% at 1649K.

The role of grain size on fluid dynamics is very small, but the amount of crystals settled down to the bottom of the magma ocean has small dependence on the grain size. If the crystal size is 1cm, 1km thickness bottom layer is formed.

The fluid dynamic regime changes into soft turbulence in 100 years in the order in the magma ocean of Vesta.

The summary of our conclusion is as follows.

(1)The pressure effect in the interior of Vesta is negligibly small.
(2)The solidification of a magma ocean of Vesta before the rheological transition follows batch solidification.
(3)The size of crystallizing grains has a minor effect on the evolution of magma ocean until the rheological transition.
(4)The mantle would be harzburgite if the interstitial melt was effectively extracted at the later soft turbulence stage.

Fig. The thickness of the bottom layer consisting of settled crystals from the main body of a magma ocean.

PPS21-01 Room:416 Time:April 29 09:00-09:15

Keywords: Vesta, magma ocean

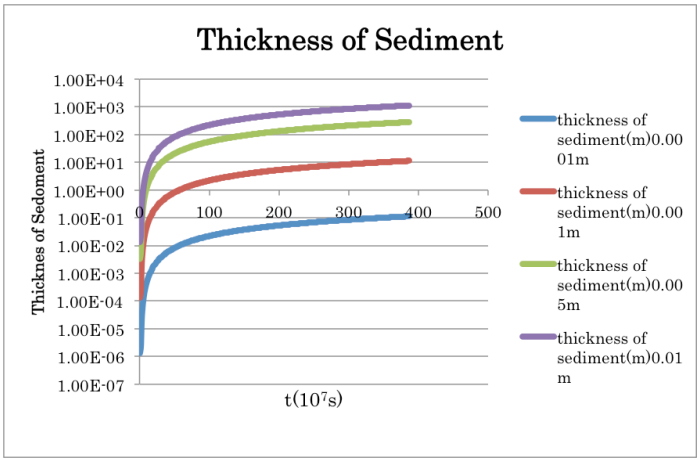

Japan Geoscience Union Meeting 2014
(28 April - 02 May 2014 at Pacifico YOKOHAMA, Kanagawa, Japan)

PPS21-02 Room:416 Time:April 29 09:15-09:30

Thermal evolution simulation of Vesta including convection and melt migration

NOGAMI, Tatsuhiko[1*] ; SIRONO, Sin-iti[2]

[1]Division of Earth and Planetary Sciences, Graduate School of Science, Nagoya University, [2]Division of Earth and Planetary Sciences, Graduate School of Science, Nagoya University

Vesta has been regarded as the parent body of the HED meteorites. From the observation of DAWN spacecraft, the uppermost layer of Vesta is composed of howardite and its thickness ranges from 50km to 80km (Jutzi et al. 2013). It is known that the ratio of the number of eucrites to diogenites is around two. Based on these facts, rapidly cooled magma layer on Vesta should be more than 10km in thickness.

In this work, I studied the evolution of internal thermal evolution of Vesta due to heating of decay of 26Al. I calculated the temperature distribution by solving numerically heat conduction equation. According to Formisano et al.(2013), if Vesta completed its formation within 1.4Ma from the injections of 26Al into the solar nebula, the degree of silicate melting inside Vesta exceeds 50 vol%. But in that work, convection and melt migration were not taken into account. These two mechanisms contribute to cool down Vesta. It is expected that the formation of Vesta should be completed earlier if these effects are taken into account. On the other hand, it is known that it takes about a few million years for Vesta-size planet to complete its formation according to the standard model of planetary formation.

As a convection model, I adopted the model of Kaula (1979). It was assumed that generated melt migrates to the surface instantaneously, and the migrating melt to the surface was accounted as the rapidly cooled magma. There are two parameters in this study, including a (the percentage of melt migration) and t0 (formation time of Vesta), and perform simulation taking into account the convection and melt migration.

As a result, convection and melt migration substantially change the evolution of internal thermal structure, and total volume of magma considerably depends on a and t0. The magma volume increases as a increases. On the other hand, the magma volume decreases as t0 increases.

When t0=0, corresponding to no decay of 26Al at the beginning, and if $a>0.3$, the erupting magma layer of 10km in thickness is formed. When a=1, corresponding to total melt migration, the magma layer of 10km is formed if $t0<0.9$Ma. According to these results, Vesta should be completed its formation within 0.9Ma after CAI formation, and more than 30% of generated melt should migrate the surface. But total generated melt migration is not reasonable . If $a<1$, Vesta has to be formed earlier than a=1.

Therefore, it is suggested that the formation time of Vesta should be earlier than the estimate by Formisano et al.(2013), and rapid formation mechanism of 100km sized objects is needed.

Japan Geoscience Union Meeting 2014
(28 April - 02 May 2014 at Pacifico YOKOHAMA, Kanagawa, Japan)

PPS21-03 Room:416 Time:April 29 09:30-09:45

Thermal conductivity measurements of sintered glass beads and application to planetesimal thermal evolution

TSUDA, Shoko[1] ; SAKATANI, Naoya[2*] ; OGAWA, Kazunori[3] ; TANAKA, Satoshi[3] ; ARAKAWA, Masahiko[4] ; HONDA, Rie[5]

[1]University of Tokyo, [2]The Graduate University for Advanced Studies, [3]Institute of Space and Astronautical Science, [4]Kobe University, [5]Kochi University

In the planetary formation process, dusts in the early solar nebula would have formed into planetesimals. Planets and asteroids have been formed by collisions of planetesimals. To constrain planetesimal ' s formation process and internal structure is an important issue. Especially, thermal evolution of planetesimal is key phenomenon for this purpose, and thermal conductivity of the planetesimal constituents is an essential parameter for understanding the thermal evolution.

As planetesimals are treated as dust aggregates, they would experience sintering when their temperature increases as a result of thermal evolution. The sintering makes neighbor particles bonded. The thermal conductivity of powered materials before sintering has been researched recently. However, thermal conductivity of sintered dust has not been measured under vacuum. Once dusts undergo the sintering, contact faces, so-called neck, are formed between dusts. The sintering causes growth of the neck and decrease of the porosity. It is thought that these changes make thermal conductivity higher than not-sintered dusts.

Based on our previous measurements of the thermal conductivity of glass beads, a positive correlation between thermal conductivity and compressional stress (thus, the inter-particle contact area) was observed with sample porosity remaining constant. Therefore, the thermal conductivity should be expressed as a function of not only porosity but also contact area between the particles.

This study aims at investigating thermal conductivity of the sintered materials under vacuum condition, in order to estimate effect of the sintering on thermal evolution of planetesimals. Especially, we focus on the dependence of neck size on the thermal conductivity.

We used three sizes of glass beads (250, 500, and 1000 μm) as analogous samples of dusts. For respective glass beads, we made three sintered samples with different degrees of sintering, or different neck size, in order to investigate the neck size dependence of the thermal conductivity. To measure the neck size, the sintered particles were separated and the neck crack size was observed using optical microscope. The thermal conductivity was measured by line heat source method under vacuum.

As a result of these experiments, we confirmed that the neck sizes of the nine samples had different ratio of neck size to beads radius, whose average values were ranged from 0.075 to 0.30. The thermal conductivity was ranged from 0.036 to 0.25 W/mK. These values were more than 10 times higher than that of not-sintered glass beads. Combining the results of neck size and thermal conductivity measurements, it was found that the thermal conductivity is proportionally related to the neck size ratio independent of the particle size. In these experiments, the porosity was constant about 40%. Therefore, when we calculate thermal evolution of planetesimals under sintering, the thermal conductivity should be estimated from the neck size at least until the neck size ratio grows up to 0.3 (initial stage of sintering).

Finally, we calculated the thermal evolution of the planetesimal using the relation of the thermal conductivity and the neck ratio we found in this experiment. Hypothesized planetesimals have radius between 100 m and 1000 m, formation age between 1 Myr and 3 Myr after CAI formation, and dust diameter of 1 and 1000 μm. As a result of the calculation, it was found that the sintering and resulting increase of the thermal conductivity make internal peak temperature more than 1000 K lower than the case when the sintering effect is not included in the calculation. In addition, internal temperature structure and neck size (or material strength) distribution in the planetesimals vary widely depending on the size and formation age of the planetesimals and particle size of dust.

Japan Geoscience Union Meeting 2014
(28 April - 02 May 2014 at Pacifico YOKOHAMA, Kanagawa, Japan)

PPS21-04 Room:416 Time:April 29 09:45-10:00

The effect of melt on frictional behavior and the implication for deep moonquake

AZUMA, Shintaro[1*] ; KATAYAMA, Ikuo[1]

[1]Department of Earth and Planetary Systems Science, Hiroshima University

Apollo program (Passive Seismic Experiment) investigated a number of seismic events in moon (e.g., Nakamura 2003). These seismic events (moonquakes) are classified to four categories; thermal moonquake, shallow moonquake, impact moonquake and deep moonquake (Latham et al., 1969). In kinds of moonquake, deep moonquake is especially interesting because the occurrence depth of deep moonquake (700?1200 km) is obviously in plastic deformation region where frictional behavior and fracture does not occur. Analysis of PSE (Passive Seismic Experiment) data and modelling in previous studies suggest that the partial melt layer underlies near the occurrence depth of deep moonquake (Weber et al., 2011). Therefore partial melt possibly is one of important factor on the deep moonquake. Here we show the results of frictional experiments using a borneol?diphenylamine which can be adjusted in melt fraction and dihedral angle (Takei 2000). When dihedral angle is 30o, frictional coefficient becomes small with decrease of melt fraction. Although frictional coefficient is significantly decreased when dihedral angle is 0o, frictional coefficient does not depend on melt fraction. When dihedral angle of partial melt is 0o, frictional behavior is fully dominated by partial melt. Partial melt is considered to have the three effects on the shear strength. First, our frictional experiments found that partial melt decrease frictional coefficient. Second, partial melt behave as the pore pressure. Third, partial melt extracts the water from the surrounded rocks, and induces the shear localization (the stress concentration). Considering these effects of partial melt on frictional behavior, partial melt might be one of important factors on deep moonquake.

Keywords: melt, deep moonquake, moon, frictional behevior

Japan Geoscience Union Meeting 2014
(28 April - 02 May 2014 at Pacifico YOKOHAMA, Kanagawa, Japan)

PPS21-05 Room:416 Time:April 29 10:00-10:15

Velocity scaling of granular convection and its application to timescale of regolith migration

YAMADA, Tomoya[1*] ; KATSURAGI, Hiroaki[1]

[1]Graduate School of Environmental Studies, Nagoya University

On the basis of accurate surface observation of asteroid Itokawa, it has been thought that regolith migration and sorting could occur [1]. Besides, Nagao et al. revealed that cosmic-ray exposure age of Itokawa's surface grains is less than 8 Myr [2]. As a possible explanation for such active and young surface of Itokawa, regolith convection caused by impact-induced seismic shaking has been considered [1]. Indeed, granular convection can be readily observed in the laboratory experiment of vertically vibrated granular matter (e.g. [3]). However, the quantitative feasibility of granular convection under the microgravity environment has not been studied well so far. Although the direct control of gravity is quite difficult, we instead employ the scaling approach to figure out the gravity dependence of granular convective velocity. Specifically, we measure the granular convective velocity under various experimental conditions. Then, using the systematically obtained data, we find a scaling relation among the convective velocity, gravitational acceleration, and other control parameters such as vibration frequency, grain size, and so on. We also estimate the timescale of regolith migration due to the granular convection by using the obtained scaling.

The grains used in this experiment are glass beads of diameter d = 0.4, 0.8, or 2 mm (AS-ONE corp. BZ04, BZ08, BZ2). The experimental setup consists of a cylinder made by plexiglass of its height 150 mm and inner radius R = 16.5, 37.5, or 75 mm. The cylindrical cell is filled by glass beads to make a granular bed of the height H = 20, 50, 80, or 110 mm. The system is mounted on an electromechanical vibrator (EMIC 513-B/A) and shaken vertically. The vibration frequency f is varied from 100 to 300 Hz and the maximum dimensionless acceleration is varied from 2 to 6. Motions of glass beads on the sidewall of the container are captured by a high-speed camera (Photoron SA-5) with a macro lens. PIV (Particle imaging velocimetry) method is used to compute the vertical component of the convective velocity, v_z. The maximum value of the velocity is nondimensionalized as $v_{zmax}/(gd)^{1/2}$, where g is the gravitational acceleration. Using the obtained experimental data, we scale $v_{zmax}/(gd)^{1/2}$ by the shaking parameter S [4] and the dimensionless system size L. S represents the energy balance between vibration and gravity, $S=(2\pi Af)^2/gd$, where A is shaking amplitude. L is the scaled system size defined by $L=(RH)^{1/2}/d$.

As a result of systematic dimensional analysis, we obtain a scaling form, $v_{zmax}/(gd)^{1/2} \sim S^{0.47}L^{0.82}$. From this scaling form, we find that the granular convective velocity v_{zmax} depends on the gravitational acceleration g as $v_{zmax} \propto g^{0.97}$ when the maximum dimensionless acceleration is fixed. This means that the granular convective velocity is almost proportional to the gravitational acceleration. We also find that the timescale of regolith migration due to the granular convection is almost independent of its roll size, by assuming that L is the dimensionless convective roll size. In the presentation, we are going to discuss the consistency between the regolith migration timescale and cosmic-ray exposure age of Itokawa's surface grains.

[1]H. Miyamoto *et al.*, Science **316**, 1011 (2007)
[2]K. Nagao *et al.*, Science **333**, 1128-1131 (2011)
[3]A. Garcimartín *et al.*, Physical Review E **65**, 031303 (2002).
[4]P. Eshuis *et al.*, Physics of Fluids **19**, 123301-1 (2007)

Keywords: granular convection, scaling analysis, gravitational acceleration, regolith migration, Itokawa

Japan Geoscience Union Meeting 2014
(28 April - 02 May 2014 at Pacifico YOKOHAMA, Kanagawa, Japan)

PPS21-06 Room:416 Time:April 29 10:15-10:30

Experimental study on impact-induced seismic wave propagating in granular materials

MATSUMOTO, Eri[1] ; YASUI, Minami[2*] ; ARAKAWA, Masahiko[1]

[1]Graduate school of Science, Kobe University, [2]Organization of Advanced Science and Technology, Kobe University

Introduction:

A seismic wave survey is a direct method to investigate the sub-surface structures of solid bodies, so we measured and analyzed these seismic waves propagated through these interiors. Earthquake and Moonquake are the only two phenomena that have been observed to explore these interiors until now, while the future surveys on the other bodies, (solid planets and/or asteroids) are now planned. To complete the seismic wave survey during the mission period, the artificial method that activates the seismic wave is necessary and the one candidate for the artificial one is a projectile collision on the target body. However, to utilize the artificial seismic wave generated on the target body, the relationship between the impact energy and the amplitude and the decay process of the seismic wave should be examined. If these relationships are clarified, we can estimate the required sensitivity of seismometers installed on the target body and the distance from the seismic origin measurable for the seismometer. Furthermore, if we can estimate the impact energy from the observed seismic wave, it is expected to estimate the impact flux of impactors collided on the target body. In this study, we carried out impact experiments in the laboratory, observed the seismic waves by accelerometers, and examined the effects of projectile properties on the amplitude and the decay process of the seismic wave.

Experimental methods:

We did impact experiments by using the one-stage gas gun at Kobe University. The projectile was a polycarbonate cylinder with the diameter of 10 mm and the height of 10 mm, and a stainless and an alumina ball with the diameter of 3 mm. The stainless and the alumina balls was accelerated with the sabot made by polyethylene. The impact velocity was $\sim$100 m/s. The target was prepared by putting 200 μm glass beads into the container with the diameter of 300 mm and the height of 100 mm, up to 80 mm depth. Three accelerometers (response frequency $<$10 kHz) were set on the target surface at different distances from the impact point. The observed seismic waves were recorded as voltage on the data logger (A/D conversion efficiency 100 kHz).

Experimental results:

We calculated the propagation velocity of seismic wave by using the traveling time from the impact point to the site of accelerometer and the impact velocity, and obtained 105 $\pm$ 15 m/s. Additionally, the relationship between the maximum acceleration, g_{max}, and the normalized distance, x/R (x: distance from impact point, R: crater radius), was determined as g_{max} =268$(x/R)^{-2.8}$. From these results, it is found that the seismic wave attenuates with similar waveform on the same target, irrespective of projectile type. The duration keeping the maximum acceleration was estimated to be $\sim$0.3 ms, and this value was almost consistent with the penetration time of projectile estimated by using the model proposed by Niimi *et al.* (2011). McGarr *et al.* (1969) studied the energy conversion efficiency from impact energy to seismic momentum and obtained the ratio of the impulse of projectile during the penetration, I, to the kinetic energy of projectile, E_k. As a result of this study, the I/E_k was obtained to be $1.6 \times 10^{-2} \pm 1.0 \times 10^{-2}$. On the other hand, McGarr *et al.* (1969), which the lexan projectile collided on the sand target with the impact velocity of 2-8 km/s, was obtained to be $6 \times 10^{-6} \pm 4 \times 10^{-6}$. This difference might be caused by the dependence of impact velocity on the energy conversion efficiency.

Keywords: impact-induced seismic wave, granular materials, decay process, planetary exploration, crater formation, accelerator

Japan Geoscience Union Meeting 2014
(28 April - 02 May 2014 at Pacifico YOKOHAMA, Kanagawa, Japan)

PPS21-07 Room:416 Time:April 29 10:30-10:45

Velocity measurements of impact jetting during oblique impacts

KUROSAWA, Kosuke[1*] ; NAGAOKA, Yoichi[1] ; HASEGAWA, Sunao[2] ; SUGITA, Seiji[3] ; MATSUI, Takafumi[1]

[1]PERC, Chitech, [2]ISAS, JAXA, [3]Dept. of Complexity Sci. & Eng., The Univ. of Tokyo

Impact jetting is a widely-known phenomenon in both hypervelocity impact experiments and hydrocode calculations. There are two important features in impact jetting, which are (1) extremely high velocity greater than the impact velocity and (2) the high degree of shock heating. Jetting has been considered as a mechanism for the origin of chondrules, tektites and impact glasses, Pluto, and the Moon. Jetting during a symmetric collision between two thin plates has been well studied. However, the understanding of jetting for spherical impactors is essential for planetary applications and it has not been obtained. One of the reasons for this is the lack of the experimental data of hypervelocity jetting of obliquely-impacted spherical projectiles. Although the temperature of jetted vapor has been investigated under a wide range of experimental conditions, only 3 data points, including unpublished data, have been reported as the jet velocity, which is one of the important anchors for developing a jetting model.

In this study, we conducted a series of oblique impact experiments using spherical projectiles and 3 different targets and investigated the jet velocity as a function of impact velocity and target materials. The frame rate of a high-speed imaging was 100 ns/frame to resolve the jetting initiation during projectile penetration. We found that the velocity ratio of the jet velocity to the impact velocity increases as the shock impedance of target increases at a given impact velocity and decreases with as impact velocity increases.

We obtained the first systematic data set for the jet velocity of spherical projectiles during oblique impacts. Using the data set, we constructed a physical model to explain the observed jet velocities. We found that (1) a classical phenomenological model constructed by Ang (1990) predicts well observed jet velocities if we use the vertical component of impact velocity instead of impact velocity in his model and that (2) observed jet velocities can be obtained by the sum of the horizontal component, the deformation velocity of the shocked projectile, and the particle velocity after isentropic release. The latter model may provide a physical basis of the jet formation

Both the standard and our physical model predict the jet velocity during oblique impacts reaches 2.5 times than the impact velocity. Although the mass of jetted materials must be small for energy conservation, the aerodynamic interaction between such hypervelocity jet and an ambient atmosphere may be significant because the heating rate of aerodynamic ablation is proportional to the cube of the velocity. In the case for an oblique impact on Titan, the jet velocity may reach 30 km/s in the case of typical cometary impacts and may generate strong EUV radiation from produced high-temperature plasma in the N2CH4 atmosphere via aerodynamic interaction near the surface of Titan. Active chemical reactions of C-bearing species may be driven by the produced EUV. The available energy source near the current Titan surface is only cosmic rays. Thus, hypervelocity jetting may be a new energy source for atmospheric chemistry on Titan.

Keywords: Hypervelocity impacts, Oblique impacts, High-speed video camera, Ultrafast imaging observation, Impact jetting, Titan

Japan Geoscience Union Meeting 2014
(28 April - 02 May 2014 at Pacifico YOKOHAMA, Kanagawa, Japan)

PPS21-08 Room:416 Time:April 29 11:00-11:15

The stability of amino acids in early ocean by meteorite impacts: Implication for chemical evolution of biomolecules

UMEDA, Yuhei[1*] ; SEKINE, Toshimori[1] ; FURUKAWA, Yoshihiro[2] ; KAKEGAWA, Takeshi[2] ; KOBAYASHI, Takamichi[3]

[1]Graduate School of Science, Hiroshima University, [2]Graduate School of Science, Tohoku University, [3]National Institute for Materials Science

Prebiotic oceans may have contained abundant amino acids, and were subject to meteorite impacts, especially during the late heavy bombardment. It has been unknown how meteorite impacts affected such dissolved amino acids in the early oceans. Experiments in the present study were performed using aqueous solutions containing olivine or hematite powders and ^{13}C-labeled glycine and alanine. In particular, the reaction products from ^{13}C-labeled amino acids are expected to compose ^{13}C, distinguishing if they are contaminants or not. Two powders of olivine and hematite help to keep the oxygen fugacity low and high during experiments, respectively in order to investigate the effect of oxygen fugacity on chemical reaction of amino acids. The run product of selected amino acids and amines in samples were analyzed with liquid chromatography-mass spectrometry (LC/MS). Some experiments were carried out in the presence of ammonia and/or benzene. The results revealed that amino acids survived partially or reacted out in early ocean through meteorite impacts. It was found that glycine changes into alanine and large amounts of methylamine and ethylamine are formed. Amine formation from alanine was increased considerably in the presence of Fe_2O_3 rather than olivine under similar impact conditions. XRD for the recovered hematite powders indicated the presence of a small amount of magnetite, suggesting that the oxygen fugacity was kept high enough to be close to the Fe_2O_3-Fe_3O_4 buffer. The formation of n-butylamine, detected as the largest number of carbon species in the recovered samples from the solutions with ammonia and benzene, suggests that chemical reactions to form new biomolecules can proceed through marine impacts. These results suggest that amino acids in early oceans can proceed further by impact-induced reactions, implying that impact energy plays a role in the prebiotic formation of various biomolecules, although the reactions depend upon the chemical environments as well.

Japan Geoscience Union Meeting 2014
(28 April - 02 May 2014 at Pacifico YOKOHAMA, Kanagawa, Japan)

PPS21-09 Room:416 Time:April 29 11:15-11:30

Organic aerosol experiments for CH_4/CO_2 atmospheres using a hydrogen/helium UV lamp

HONG, Peng[1*] ; SEKINE, Yasuhito[1] ; SUGITA, Seiji[1]

[1]Complexity Sci. & Eng., Univ. of Tokyo

Organic aerosols are photochemically produced in CH_4-rich reducing atmospheres, but their production mechanisms are not well constrained. Organic aerosol layers are believed to influence the surface temperature of early Earth, through its anti-greenhouse (Pavlov et al., 2001) and/or indirect greenhouse effects (Wolf and Toon, 2010), however, because of the uncertainty of the aerosol production mechanism, there are large uncertainties inherent in previous estimates of the aerosol production rate and optical depth of aerosol layers (Trainer et al., 2006). In order to put a constraint to the production mechanism and obtain aerosol production rate applicable to CH_4/CO_2 atmospheres, we conducted laboratory experiments to form organic aerosol analogues using a hydrogen/helium lamp that simulates solar far UV (FUV) with wavelengths longer than 110 nm. We measured the aerosol production rate as functions of UV flux and of CH_4/CO_2 ratio in the reactant gas. The aerosol production rates were determined by ellipsometrically measuring the growth rates of thin organic films deposited on a substrate. The UV fluxes from the hydrogen/helium lamp were measured by N_2O/CO_2 actinometry. Our experimental results show that the aerosol production rate is not a second-order function but a linear function of UV flux. This leads to a lower estimate for aerosol production rate due to FUV irradiation, when extrapolating the production rate in Titan's atmosphere to early Earth and exoplanets. We also found that the aerosol production exhibits a steep decrease when the CH_4/CO_2 ratio becomes less than unity. In order to interpret the dependence of aerosol production rate on the CH_4/CO_2 ratio, we also performed one-box photochemical calculations, including 791 reactions and 134 species up to C_8 hydrocarbons. The one-box photochemical model was validated against some basic carbon species (CH_4, C_2H_2, C_2H_4, C_2H_6, CO, CO_2), in which the abundances of those species calculated with the model and observed with a quadruple mass spectrometer (QMS) show a good agreement. We found that the observed production rate is in a good agreement with polymerization reaction rates involving aromatic hydrocarbons (i.e., benzene), suggesting benzene is the key parent molecule controlling the aerosol production. On the other hand, polymerization reactions involving polyynes do not account for the experimental data, suggesting that they are not the limiting molecules. This implies that aerosol production rate in an early Earth atmosphere due to solar FUV would become significantly lower than a previous estimate which includes polymerizations of polyynes as formation reactions of aerosols (Pavlov et al., 2001), resulting in an optically thinner aerosol layer by a factor of 100. Thus the optical depth of organic aerosol layers produced by solar FUV in an early Earth atmosphere would not have had efficient anti-greenhouse effect or indirect greenhouse effect, which makes other greenhouse effect important for the Archean climate, such as greenhouse effect of ethane. We will also discuss the possibility of aerosol formation through nitrile reactions driven by high-energy particle irradiation, which could be more efficient than the aerosol production due to solar FUV.

Keywords: organic aerosol, photochemistry, laboratory experiment, reducing atmosphere

Japan Geoscience Union Meeting 2014
(28 April - 02 May 2014 at Pacifico YOKOHAMA, Kanagawa, Japan)

PPS21-10 Room:416 Time:April 29 11:30-11:45

Proto-atmosphere on giant icy satellites forming within gaseous circum-planetary disks

MIKAMI, Takashi[1*] ; KURAMOTO, Kiyoshi[1]

[1]Department of Cosmosciences, Graduate School of Science, Hokkaido University

In spite of the great similarity in size and mean density, the giant icy satellites Ganymede, Callisto, and Titan have very different surface environments. In particular, only Titan holds a thick atmosphere dominated by N_2. Recent data of the Cassini spacecraft indicated that atmospheric N_2 is probably originated from other nitrogen-bearing species like NH_3. However, it still remains an open question when and how N_2 was generated. This is partly because the physical states of giant icy satellites have been poorly understood.

According to a widely-accepted theory of regular satellites formation, the giant icy satellites were formed in subnebulae with low temperature and low pressure taking a long accretion time. Some models assert that their surfaces were kept too cold to induce significant differentiation during accretion. However, these satellites may capture a significant amount of subnebula gas, which possibly forms proto-atmospheres along with gases volatilized from icy components. Such a hybrid-type proto-atmosphere may have significant blanketing effect.

Here, we numerically analyze the structure and effect of a hybrid-type proto-atmosphere. Our model atmosphere is hydrostatically connected with subnebula at the satellite Hill radius. It contains H_2 and He as nebula gas components, H_2O and NH_3 as volatilized ice components. The radiative-convective equilibrium structure is solved as a function of surface temperature. The subnebula conditions are given by Canup and Ward (2002), the temperatures are 150 K at Ganymede, 120 K at Callisto, and 50 K at Titan, and the corresponding subnebula pressures are varied over 0.1-10 Pa.

For all the boundary conditions, the proto-atmosphere is opaque due to water vapor, so that the outgoing thermal radiation (OTR) flux at top of the atmosphere is smaller than that of black body radiation without atmosphere when the surface temperature is higher than 273 K. When the surface temperature is lower, the OTR fluxes from the proto-atmospheres of Ganymede and Callisto are close to black-body radiation because these atmospheres have low surface pressure and are optically thin due to large scale height under high background temperature. On the other hand, the proto-atmosphere of Titan has another type of solution with the OTR fluxes significant lower than blackbody radiation under low surface temperature. This is due to the formation of optically thick atmosphere tightly bounded by gravity because of low background temperature.

These results imply that a warm proto-atmosphere near 200 K could be kept on Titan for a long time after the end of accretion. Our stability analysis suggests that the proto-atmospheres of Ganymede and Callisto were lost associated with the dissipation of the Jovian subnebula, but that of Titan survived after the dissipation of the Saturnian subnebula.

In the case, NH_3 vapor pressure would be kept high under the irradiation of the solar UV for a long time. The present atmospheric N_2 of Titan may be generated by photochemical reaction of NH_3 vapor in such a warm proto-atmosphere.

Keywords: Giant icy satellite, Atmosphere, Circum-planetary disk

Japan Geoscience Union Meeting 2014
(28 April - 02 May 2014 at Pacifico YOKOHAMA, Kanagawa, Japan)

PPS21-11 Room:416 Time:April 29 11:45-12:00

Atmospheric formation and thermal evolution of a proto-Mars growing in the solar nebula

SAITO, Hiroaki[1*] ; KURAMOTO, Kiyoshi[1]

[1]Cosmo Sci., Hokkaido Univ

It is widely accepted that Mars is a survivor of proto-planets formed by oligarchic growth i.e., the runaway accretion of planetesimals. Numerous planetesimals impacts onto the growing proto-Mars likely cause shock-melting, resulting into the early core formation as constrained by the chronology of Martian meteorites. Such impacts should also induce the degassing of H_2O and other molecular species from accreting materials, which contributes to atmosphere formation. Since the oligarchic growth proceeds within the solar nebula, a growing Mars probably acquired a proto-atmosphere consisting of the mixture of nebula gas component and degassed component. Such a hybrid-type proto-atmosphere may play important role in thermal balance and volatile partitioning between the planetary surface and interior. However, the structure and behavior of such atmosphere has been poorly investigated so far.

In this study, we build a one-dimensional radiative-convective (RT) equilibrium model for a hybrid-type proto-atmosphere assuming a compositional double layer structure. Here the upper layer is dominated by H_2-He continuing from the solar nebula and the lower one is dominated by degassed components enriched in H_2O. Radiative transfer is modeled, taking into account the absorptions by H_2, He and H_2O. RT equilibrium structures are obtained as a function of thermal luminosity that would be balanced with accretional heating rate and the amount of degassed component. The degassed component consists of H_2O and H_2 with molar ratio 1:5 in equilibrium with metal and silicate. The accretion time is taken 10^6-10^7 years.

For the pure H_2-He atmosphere, the surface temperature is kept lower than 700 K. Supply of degassed component increases the surface temperature that can exceed 1500 K given the mass of degassed component more than 1% of the Mars mass. If planetesimals contain enough proportions of H_2O and other heavy volatiles, growing Mars would have global magma ocean sustained by the blanketing effect of proto-atmosphere. This would promote core formation and transport of dissolved volatiles.

Japan Geoscience Union Meeting 2014
(28 April - 02 May 2014 at Pacifico YOKOHAMA, Kanagawa, Japan)

PPS21-12 Room:416 Time:April 29 12:00-12:15

Line-by-line calculations of radiation properties for exoplanets with steam atmosphere

ONISHI, Masanori[1*] ; HASHIMOTO, George[2] ; KURAMOTO, Kiyoshi[3] ; TAKAHASHI, Yoshiyuki O.[1] ; TAKAHASHI, Yasuto[3] ; ISHIWATARI, Masaki[3] ; HAYASHI, Yoshi-yuki[1]

[1]Department of Earth and Planetary Sciences, Kobe University, [2]Department of Earth Sciecnes, Okayama University, [3]Department of Cosmosciences, Graduate School of Science, Hokkaido University

For a hot water rich atmosphere, there is an upper limit on the thermal emission that is unrelated to surface temperature (Simpson, 1927, Nakajima et al., 1992). The radiation limit is deeply related to evolution of planetary atmosphere. Hamano et al., 2013 showed that terrestrial planets can be divided into two distinct types on the basis of their evolutionary history during solidification from the initially hot molten state depending on whether incoming flux from a host star is larger or less than the radiation limit. On the other hand, the first direct image of an exoplanet has finally occurred in 2004 (Chauvin et al., 2004), it is expected to observe radiation spectrum from terrestrial planets near future. If we can observe the spectrum, we have potential to clarify the atmospheric and surface environment and history of the planets. In order to estimate the planetary environment from the observation, numerical simulation of radiative transfer is needed. The most reliable calculation method of the radiation is line-by-line treatment. Goldblatt et al., 2013 calculates the radiative transfer of a pure water atmosphere by line-by-line treatment. Goldblatt et al., 2013 investigates only one case of surface water amount, one current ocean mass case. In this study, we calculate the radiative transfer in steam atmosphere by line-by-line treatment in several surface water amount cases.

Absorption cross section of water vapor was calculated from HITEMP2010 (Rothman et al., 2010) and MT_CKD continuum model (Mlawer et al., 2012). We used a 1D convective model in pure water atmosphere. The surface temperature was varied from 250 to 2000 K. The total water amount of water was varied from 0.01 to 5 current Earth ocean mass (270 bar). For rapid calculation, we prepared absorption cross section table and calculated required absorption cross section by cubic spline interpolation. A two-stream approximation (Toon et al., 1989) was used to calculate radiative transfer by line-by-line treatment with resolution of 0.01 cm^{-1} wavelength.

A radiation limit of our study is 282 W m^{-2}. The value is good agreement with that of Goldblatt et al., 2013. When the total water amount is lesser, increasing of outgoing thermal flux over radiation limit occurs in lower surface temperature conditions. In 0.01 current ocean mass condition, increasing of flux occurs in lower than 1000 K. In this case, most of flux radiate from 10 micron and 4 micron window region. Results of optical depth calculation indicate that we can't detect NIR and IR radiation from the surface of planets with surface temperature higher than 1500 K, even if the planet has 0.01 water amount.

Keywords: steam atmosphere, radiative property, radiation limit

Japan Geoscience Union Meeting 2014
(28 April - 02 May 2014 at Pacifico YOKOHAMA, Kanagawa, Japan)

PPS21-13 Room:416 Time:April 29 12:15-12:30

Dependence of the runaway threshold on water distributions on the surface of Earth-like planets

NITTA, Akira[1*] ; ABE, Yutaka[1] ; O'ISHI, Ryouta[2] ; ABE-OUCHI, Ayako[2]

[1]Department of Earth and Planetary Science, Graduate School of Science, University of Tokyo, [2]Atmosphere and Ocean Research Institute, University of Tokyo

Liquid water is one of the most important material not only for its large effect on planetary climate but also as a controlling factor of the habitability [e.g. Kasting et al., 1993]. Water planets, which are planets with liquid water on their surface, can be divided in 3 types: 'ocean planets', 'partial-ocean planets', and 'land planets'. Ocean planets have enough water to cover their surface entirely. Partial-ocean planets, which are like the Earth, have an interconnected ocean and lands. Land planets have little water in scattered lakes around both Poles [Abe et al., 2013, Hawaii, Kona]. The type of the water planet is determined by the balance between the surface water transport, which depends on the amount of water and topography, and the atmospheric water transport, which depends on the global circulation.

Surface water on each water planet is unstable and entirely vaporized when the planet receives insolation above a certain critical value. It is because of the positive feedback of the greenhouse effect of water vapor. This phenomenon is called the runaway greenhouse. In the following, the critical insolation is called 'runaway threshold' [e.g. Abe and Kasting 1988; Nakajima et al, 1992; Kopparapu et al., 2011].

Abe et al. [2011] discussed the difference of the runaway threshold between Earth-sized ocean planets and land planets using a 3-D model for the first time. They found that the surface water of land planet is significantly stable than that of ocean planet against the large insolation. While an ocean planet gets unstable and the runaway greenhouse occurs when the insolation reaches about 130% of that on the present Earth, a land planet remains stable until the insolation reaches 170%. However, a land planet that they represented is only one of the various situations of land planets, and they didn't mention the effect of variety of surface water distributions on the planetary climate.

Takao [2013] showed the dependence of the runaway threshold on latitudinal surface water distribution using the combination of meridional energy balance model (EBM) and the vertical radiative-convective equilibrium model. He suggested that runaway threshold of the Earth-sized water planet varies with the degree of latitudinal localization of surface water. Nevertheless, his 1-D EBM was so simple that he could neither discuss about the effects of longitudinal distribution of surface water, nor include dynamical global circulation.

In this study, we perform numerical experiments to clarify the effects of the surface water distribution on runaway threshold of Earth-sized planets with a 3-D model, GCM.

We use CCSR/NIES AGCM 5.4g [Numaguchi, 1999], which includes dynamical atmospheric circulation, radiative transfer, formation of clouds, and so on. While this model is adapted to the present Earth, it cannot calculate the change of surface water distribution determined by the water amount and topography. Therefore, we assumed the surface water distribution, which is determined as a result of the balance between the surface and atmospheric water transport in reality, and used it as the boundary condition. Then, we raised the insolation gradually until the surface water got unstable for each surface distribution, and evaluated the runaway threshold.

We found that the degree of localization of surface water significantly affects the runaway threshold, and it varies from 180% (extremely localized land planet) to 130% (ocean planet) continuously. Even if no surface water is given low latitudes area initially, because the Hadley circulation transports water to such area, when the initial surface water area reaches adequately low latitudes, the runaway threshold is almost the same as that of ocean planets, that is, 130%. We also investigated the dependence on the longitudinal water distribution. As a result, even if the total area of surface water is the same, there are about 10% of differences in the runaway threshold depending on its distribution.

Keywords: runaway greenhouse, GCM, Earth-like planet

Japan Geoscience Union Meeting 2014
(28 April - 02 May 2014 at Pacifico YOKOHAMA, Kanagawa, Japan)

PPS21-14 Room:416 Time:April 29 14:15-14:30

Dead zones by electric heating in protoplanetary disks

MORI, Shoji[1*] ; OKUZUMI, Satoshi[1]

[1]Tokyo Institute of Technology

Turbulence driven by magnetorotational instability (MRI) is a viable mechanism of angular momentum transport in accretion disks. In protoplanetary disks, however, there is a region where the ionization degree is too low for MRI to be active (e.g., Gammie 1996; Sano et al. 2000). Whether turbulence is present or not strongly affects the growth of dust particles to planetesimals. Therefore, a good knowledge of the size of dead zones is essential to understanding planet formation.

In this study, we focus on the heating of electrons by turbulent electric fields and its effect on the ionization state of protoplanetary disks. Previous studies have assumed that electrons in the disks have the same temperature as the neutral gas. However, this is not necessarily the case in MRI-driven turbulence, in which turbulent electric fields can significantly heat up electrons (Inutsuka & Sano 2005). Heated electrons efficiently adsorb onto dust grains, and therefore electron heating leads to a reduction of the ionization degree (Okuzumi & Inutsuka, in prep.). This could effectively increase the dead zone size by reducing the saturation level of MRI turbulence outside the conventional dead zone.

The aim of this study is to show where in protoplanetary disks the effect mentioned above becomes important. We calculate the ionization degree of disks assuming that MRI operates outside the dead zone. For a minimum-mass solar nebula with the dust grain radius of 0.1um and dust-to-gas mass ratio of 0.01, we find that the effect becomes significant in a region extending from the outer edge of the dead zone (at ˜20 AU from the central star) out to 70 AU. Furthermore, our analytic estimate suggests that the saturation level of turbulence in this region is significantly low.

Keywords: protoplanetary disk, ionization degree, dust grains, MHD turbulence, electric heating

Japan Geoscience Union Meeting 2014
(28 April - 02 May 2014 at Pacifico YOKOHAMA, Kanagawa, Japan)

PPS21-15 Room:416 Time:April 29 14:30-14:45

Collisional disruption of sintered dust aggregates

SIRONO, Sin-iti[1*] ; UENO, Haruta[1]

[1]Graduate School of Environmental Sciences, Nagoya University

Planets are formed in a protoplanetary nebula consisting of gas and dust grains. The first step of planetary formation is coagulation of dust grains, leading to the formation of dust aggregates. Further growth of the dust aggregates is promoted by mutual collisions between them. The motion of dust aggregates gradually decouples from that of the gas as aggregates grow. Dust aggregates drift inward due to gas drag. If the inward drift is faster than aggregate growth, solid components in a protoplanetary nebula disappears and planets cannot be formed. To prevent infalling, many mechanisms have been proposed (Kretke & Lin 2007, Lyla et al.2009, Sandor et al.2011). Fast collisional growth during the infalling of icy dust aggregates (Okuzumi et al. 2012) is another possibility. These studies are based on the assumption that the motion of aggregates decouples from gas. The infalling velocity is on the order of 1m/s when substantial decoupling is attained. Aggregates should grow to the sizes corresponding to the infalling velocity. Is it possible?

Experimentally, collisional breakup velocity of micron-sized SiO2 dust aggregates is on the order of 1m/s(Blum 2010). Breakup velocity for H_2O ice aggregates is also on the same order(Shimaki & Arakawa 2012). However, it is difficult to produce highly porous dust aggregates experimentally due to the Earth's gravity. I conducted two-dimensional numerical simulation of sintered dust aggregates in this study. It has been pointed out that sintering of H_2O ice proceeds in wide region of a protoplanetary nebula (Sirono 2013). As sintering proceeds, a neck between adjacent grains grows and mechanical interactions between grains greatly change. The effects of sintering are taken into account by changing breaking forces of a contact. The interactions between non-sintered contacts (Dominik & Tielens 1997) are adopted for newly formed contacts.

If sinterng proceeds sufficiently such that a neck is disappeared, catastrophic disruption was observed at low collision velocities (˜10cm/s). This is because a contact is broken by rolling of a grain. On the other hand, catastrophic disruption at low collision velocities was not realized for less-sintered aggregates. This is due to immediate reconnection between grains with a non-sintered mode. These results depends on the tensile strength of H_2O ice. The breakup velocity increases as the strength increases. From the results obtained in this study, the evolution of icy dust aggregates is various, depending on the location in a protoplanetary nebula.

Keywords: dust aggregate, protoplanetary nebula, collisional disruption, sintering

Japan Geoscience Union Meeting 2014
(28 April - 02 May 2014 at Pacifico YOKOHAMA, Kanagawa, Japan)

PPS21-16 Room:416 Time:April 29 14:45-15:00

Planetesimal size and protoplanetary disk turbulence

KOBAYASHI, Hiroshi[1*] ; TANAKA, Hidekazu[2] ; OKUZUMI, Satoshi[3]

[1]Nagoya University, [2]Institute of Low Temperature Science, Hokkaido University, [3]Tokyo Institute of Technology

When the random velocities of bodies are greater than their surface escape velocities, the runaway growth of bodies occurs, which produces a single large bodies surrounded by leftover bodies in each annual of a protoplanetary disk. The slope of the size distribution of bodies becomes steeper through runaway growth. The slope of runaway growth is seen in the size distribution of 100km sized or larger bodies in the main belt. Since the random velocities rises by turbulent stirring in the disk, the planetesimal size above which runaway growth occurs is determined by the strength of turbulence. We discuss turbulence strength in the solar nebula.

Keywords: Planetesimal, Protoplanetary disk, Asteroids, The size distribution of bodies, Planet formation

Japan Geoscience Union Meeting 2014
(28 April - 02 May 2014 at Pacifico YOKOHAMA, Kanagawa, Japan)

PPS21-17 Room:416 Time:April 29 15:00-15:15

The formation of gas planets from cores in type I migration

MAESHIMA, Naohiko[1*] ; WATANABE, Sei-ichiro[1]

[1]Division of Earth and Planetary Sciences, Graduate School of Science, Nagoya University

Many gas planets have been discovered. The formation of the gas planets requires that solid planets, which correspond to cores of gas planets, must achieve the critical core mass M_{crit} before the disk gas have entirely diffused. The cores moves radialy by torques caused by interaction with disk gas (type I migration). It was long thought that the cores fall into the star with very short timescale before achieveing M_{crit} by strong negative torque (Ward 1997, Tanaka et al. 2002). Recent study have showed that the region where positive torque operates is formed on the disk by corotation torque if we consider the non-isothermal process of the gas (Baruteau & Masset 2008,Paardekooper & Papaloizou 2008). As a result, equilibrium radii, where torque is zero, are created. The cores may accrete gas without falling into the star if they are trapped by equilibrium radius because the timescale of radial migration slows down to that of disk evolution. However, positive torque only operates for cores in limited mass range ($M_{p,min}<M_p<M_{p,max}$). If it takes long time for achieving $M_{p,min}$, the cores moves inward largely by negative torque. In this study, we examine how the orbit and mass of cores evolve depending on the disk model, and find the condition the disk must have for the gas planet formation.

The distribution of the gas surface density evolves by viscous diffusion and photoevaporation. The temperature distribution is determined by viscous heating and stellar irradiation. In the disk, an equilibrium radius is formed on the region where the main heating source shifts from the viscous heating to stellar irradiation. In this study, we investigate the possibility of the formation of gas planets at the equilibrium raidus. Cores grow by accreting planetesimals in their gravitational radius, and capture the disk gas if they achieve M_{crit}.

We find that the condition of gas planet formation is determined as follows. In diks evolving fast (α parameter of viscosity = 0.005), cores born in the middle region ($\sim$ 10AU) is captured by the equilibrium radius and capture the disk gas by achieving M_{crit} if core growth stars at the time when disk mass is still large (initial mass accretion rate $\sim 10^{-7} M\odot yr^{-1}$) and the ingredient of the cores is abundant (ratio of the solid material to gas is large $>$0.03). On the other hand, in the disks evolving slowly (α = 0.001), gas planets can be formed even if core growth stars at the stage when disk mass has been decreased (initial mass accretion rate $\sim 10^{-8} M\odot yr^{-1}$). In this case, the dependence on the ratio of the solid to gas is very weak.

Keywords: type I migration

Japan Geoscience Union Meeting 2014
(28 April - 02 May 2014 at Pacifico YOKOHAMA, Kanagawa, Japan)

PPS21-18 Room:416 Time:April 29 15:15-15:30

Protoplanet Spin by Planetesimal Accretion

SHIBATA, Takashi[1*] ; KOKUBO, Eiichiro[2]

[1]University of Tokyo, [2]National Astronomical Observatory of Japan

In the standard scenario of planet formation, protoplanets or planetary embryos are formed through runaway and oligarchic growth of planetesimals. We investigate the spin parameters of protoplanets using N-body simulations. By N-body simulations we can calculate consistently the orbital, accretionary, and spin evolution of planetesimals. The spin of protoplanets are important for terrestrial planet formation since it affects the accretion condition of protoplanets and determines the spin of terrestrial planets. For the standard model of a planetesimal disk, a Mars-sized protoplanet forms in 0.5 million years around 1 AU. We find that the spin angular velocity of planetesimals decreases as their mass increases. Planetesimals obtain their spin angular momentum on the early stage of accretion where their mass ratio is not so large. Once a runaway-growing planetesimal (protoplanet) becomes large enough, it mainly accretes smaller planetesimals whose collisional angular momentum tends to cancel out since they collide from random directions. Thus the protoplanet increases its mass but not the spin angular momentum, which leads to smaller angler velocity for larger protoplanets. When a protoplanet reaches the isolation mass, its typical spin angular velocity is as high as 10% of the critical angular velocity for rotational instability under the assumption of perfect accretion in collisions. We find that the obliquity of planetesimals is well expressed by an isotropic distribution. During the protoplanet growth, the scale height of the planetesimal system is much larger than the size of planetesimals. Thus, collisions are three-dimensional and isotropic, which leads to the isotropic obliquity distribution. We show the dependence of the spin parameters on the initial planetesimal system parameters. The spin angular velocity increases with the bulk density of planetesimals. The dependence of the spin angular velocity on the planetesimal mass becomes weaker as the initial mass of planetesimals increases. However, these system parameters do not affect the obliquity distribution.

Japan Geoscience Union Meeting 2014
(28 April - 02 May 2014 at Pacifico YOKOHAMA, Kanagawa, Japan)

PPS21-19 Room:416 Time:April 29 15:30-15:45

Gravitational accretion of particles onto moonlets embedded in Saturn's rings

YASUI, Yuki[1*] ; OHTSUKI, Keiji[1] ; DAISAKA, Hiroshi[2]

[1]Department of Earth and Planetary Sciences, Kobe University, [2]Graduate School of Commerce and Management, Hitotsubashi University

Collision and gravitational accretion of particles is an important issue related to the origin of ring-satellite systems of giant planets in the solar system. The Hill radii of Pan, Daphnis, Atlas, and Prometheus are found to be within 15 % of the observed long axes of these satellites given by the best-fit model ellipsoids. Also, the densities of these satellites (0.4 - 0.6 g cmˆ-3) are very low compared to the density of water ice and all approximately equal to the critical density at that distance, which is defined as the density of a body that entirely fills its Hill sphere. From these results, the small satellites within the orbit of Pandora are thought to be formed by accretion of small porous ring particles onto large dense cores, and further accretion seems to have been suppressed when the density of the satellite reaches the critical density at that distance. Local N-body simulations also demonstrated that a Hill sphere-filling body is produced by accretion of small porous particles onto a large dense core. However, it has not been studied how the degree of particle accretion onto moonlets in the inner parts of Saturn's rings depends on the distance from Saturn.

The shapes of these small ringmoons would also provide clues to the dynamical evolution of Saturn's rings. The fact that the shapes of these ringmoons approximately match those of their associated Hill sphere suggests that the moonlet cores were surrounded by a number of particles when they were formed. On the other hand, Pan and Atlas have the characteristic shapes with equatorial ridges, and are thought to be formed by two stages. First, their precursors whose shapes are similar to their Hill sphere without equatorial ridges were formed when the rings were thick. Then, equatorial ridges were formed through particle accretion onto the equatorial planes of the above formed objects after the rings became sufficiently thin and also before ring particles diffused. However, effects of dynamical properties of the rings on the shaping of moonlets formed by particle accretion have not been examined in detail.

Propeller-shaped structures have also been found in Cassini images of Saturn's rings. These propeller-shaped features are explained by gravitational interaction between ring particles and unseen embedded moonlets. From these observations, the sizes and orbital distributions of these unseen embedded moonlets are obtained, and such information provide us with clues to the evolution of the ring-satellite system. The propeller-shaped structures are mainly observed in the A ring. Recently, observations of similar structures have also been reported for the Cassini Division, and the B and C rings. Although some of these moonlets either may be collisional shards resulting from the breakup of a bigger icy progenitor ring body or may have formed by accretion of small low-density ring particles onto larger dense fragments, the origin of these moonlets is not clear.

Using local N-body simulation, we examine gravitational accretion of ring particles onto moonlets in Saturn's rings. We find that gravitational accretion of ring particles onto moonlets is unlikely to occur at radial locations interior to the outer edge of the C ring, unless the density of the moonlets is much larger than that of water ice or non-gravitational cohesive forces play a major role. Detailed analysis of accretion process of individual particles onto moonlets shows that particle accretion onto high-latitude regions of the moonlet surface occurs even if the rings' vertical thickness is much smaller than the moonlet's radius. The degree of particle accretion in outer rings is found to depend significantly on rings' vertical thickness and optical depth. Our results suggest that large boulders recently inferred from observations of transparent holes in the C ring are likely to be collisional shards, while propeller moonlets in the A ring would be gravitational aggregates formed by particle accretion.

Keywords: gravitational accretion, moonlet, Saturn's rings

Japan Geoscience Union Meeting 2014
(28 April - 02 May 2014 at Pacifico YOKOHAMA, Kanagawa, Japan)

PPS21-20 Room:416 Time:April 29 16:15-16:30

Mass-Loss Evolution of Super-Earths: Constraints on Their Compositions and Origins

KUROKAWA, Hiroyuki[1*] ; KALTENEGGER, Lisa[2] ; NAKAMOTO, Taishi[3]

[1]Nagoya University, [2]Max Planck Institute for Astronomy, [3]Tokyo Institute of Technology

Recent progress of he search for exoplanets, for example the transit observations with Kepler space telescope, has pushed toward small planets. Especially, ”Super-Earths”, that are planets having sizes from Earth to Neptune, are revealed as quite common: ˜30% of solar-type stars have super-Earths (Howard et al., 2012). Therefore, an understanding of their compositions, which is related to their origins, is important for planet formation and evolution.

We can speculate the compositions of super-Earths both whose masses and radii are known by using theoretical mass-radius relations for different compositions. Some fraction of super-Earths have low density, which suggests the presence of H/He envelopes formed by protoplanetary-disk gas capture. There exist. on the other hand. high-density super-Earths possibly having rocky- or water-rich compositions. The origin of this dichotomy is one problem that we address in this study, which possibly arises from the difference of the amount of captured disk gas due to different masses and disk temperature in their formation stages, or from XUV (X-ray and EUV)-driven atmospheric escape in later evolution stages (e.g., Lopez et al., 2012). Another problem that we address in this study is ”the degeneracy of composition”: The compositions of super-Earths can be fitted by various ratios of H/He envelope, rock, and water. Their atmospheric compositions have been speculated by measuring their transmission spectra, but recent observations using Hubble Space Telescope suggested that cloudy atmospheres of super-Earths (Kreidberg et al., 2014; Knutson et al., 2014). If clouds are common in atmospheres of Super-Earths, direct measurements of their compositions are difficult because clouds obscure any features of atmospheric species.

In this study, we show constraints on these problems of compositions and origins of super-Earths by calculating their mass-loss evolution due to XUV-driven atmospheric escape considering the differences of host-stellar types. The ratio of XUV luminosity and bolometric luminosity differs among stellar types, which enables us to distinguish formation origin and mass-loss origin of the dichotomy of super-Earths with or without H/He envelopes. Also, the degeneracy of compositions can be solved by considering stability criteria to lose H/He envelopes.

We calculated the critical orbital radii to lose H/He envelopes for different stellar types, that corresponds to different equilibrium temperature depending on stellar types. The obtained critical separations are consistent with the distribution of the observed super-Earths with or without H/He envelopes, suggesting that the observed dichotomy has a mass-loss origin.In this case, we expect that super-Earths having moderate density and orbiting inside the critical separation are water-rich super-Earths without H/He envelope.

We also evaluated uncertainty caused by mass-loss model and XUV luminosity and discuss the validity of our results.

Keywords: exoplanet, atmospheric escape, composition, super-Earth

Japan Geoscience Union Meeting 2014
(28 April - 02 May 2014 at Pacifico YOKOHAMA, Kanagawa, Japan)

PPS21-21 Room:416 Time:April 29 16:30-16:45

Exoplanet exploration for brown dwarfs with infrared astrometry

YAMAGUCHI, Masaki[1*] ; YANO, Taihei[1] ; GOUDA, Naoteru[1]

[1]National Astronomical Observatory of Japan

The astrometry is one of the oldest method for the exoplanet exploration. However, only one exoplanet has been found with the method. This is because the planet mass is sufficiently smaller than the mass of the central star, so that it is hard to observe the fluctuation of the central star by the planet. Therefore, we investigate the orbital period and mass of planets which we can discover by the future astrometric satellites for brown dwarfs with the mass less than a tenth of the solar mass.

So far five planetary systems have been found, whose mass ratios are larger than a tenth. For example, for the system whose distance, orbital period and mass ratio are 10 pc, 1 year and a tenth, respectively, the apparent semi-major axis reaches 3 milli-arcsecond, which can be well detected with the future astrometric satellites such as Small-JASMINE and Gaia. With these satellite, we can discover even super-Earth for the above system.

We further investigate where in the period-mass plane we can explore the planet for individual brown dwarf with Small-JASMINE and Gaia. As a result, we find that we can explore a wide region where period and mass are within 5 years and larger than 3 earth mass. In addition, we can explore the region around 0.1 day and 10 jovian mass, where planets have never found for any central star, and where we can explore only with Small-JASMINE for most target brown dwarfs.

Keywords: astrometry, brown dwarf, exoplanet exploration, infrared, Small-JASMINE, Gaia

Japan Geoscience Union Meeting 2014
(28 April - 02 May 2014 at Pacifico YOKOHAMA, Kanagawa, Japan)

PPS21-22 Room:416 Time:April 29 16:45-17:00

Experimental study on organic aerosol formation in super-Earths' atmosphere: Implications for transit observations

KOBAYASHI, Jumpei[1*] ; SEKINE, Yasuhito[2] ; HONG, Peng[2]

[1]Dept. Earth & Planet. Sci., Univ. Tokyo, [2]Dept. Complexity Sci. & Engr., Univ. Tokyo

A super-Earth is an extrasolar planet with a mass greater than Earth and below Neptune. Although there is no super-Earth in our solar system, astronomical observations demonstrate that it is one of the major categories of planets beyond the solar system. Recent transit observations of super-Earths, including GJ 1214b, indicate that their atmospheres contain opaque clouds or haze at high altitudes. One candidate for the opaque materials is metallic or salt dusts, such as KCl and ZnS, which would condense in the upper atmospheres of super-Earths. Another candidate is organic haze, such as those observed in the atmosphere of Saturn's moon Titan, which would be composed of high-molecular-weight hydrocarbon aerosols produced through photochemical reactions involving CH_4. Given the proposed formation mechanisms of nearby super-Earths, e.g., planetary migration, they would have a wide variety in chemical composition of atmosphere. However, previous laboratory experiments have mainly focused on organic aerosol formation in Titan's and early Earth's atmospheres. Thus, both the formation rate and optical property of organic haze for various atmospheric compositions have been poorly constrained by laboratory experiments.

In this study, we investigate the formation rate and optical property of organic aerosols formed by laboratory experiments simulating super-Earths' atmospheres with a wide variety in chemical composition. We used initial gas mixtures of H_2 and CH_4 or CO_2 and CH_4, and varied the H_2/CH_4 or CO_2/CH_4 ratios. The experiments were conducted at a total pressure of 1 Torr in a flow system. Cold plasma irradiation was used to initiate aerosol formation. We measured the aerosol formation rate, chemical compositions of intermediate gas molecules, and optical property of aerosol using a spectroscopic ellipsometer, a quadrupole mass spectrometer, and a UV/VIS spectrometer, respectively.

Our experimental results show that the aerosol formation rate decreases with increasing the H_2/CH_4 ratio, suggesting that recycling of high-molecular-weight hydrocarbons to CH_4 occurs through reactions with H and H_2 under H_2-rich conditions. We also show that organic aerosols are produced less efficiently at higher CO_2/CH_4 ratios. The results of gas analyses also show that formation of high-molecular-weight hydrocarbons are inhibited at higher CO_2/CH_4 ratios. These results indicate that oxygen-bearing molecules and radicals formed by CO_2 dissociation oxidizes hydrocarbons produced from CH_4, which results in a lower aerosol formation rate at higher CO_2/CH_4 ratios. Optical constant of the aerosols formed under the conditions simulating super-Earths' atmospheres is significantly lower than those of Titan aerosol analogs.

Based on the experimental results, we discuss the chemical composition and formation process of transiting super-Earths, such as GJ 1214b, by comparing the observed transmittance spectra with the model spectrum. We suggest that organic aerosol production in a H_2-rich or CO_2-rich atmosphere is inefficient so that organic haze would not be capable of explaining the observed transit spectra of super-Earths, even if they contains gaseous CH_4 in the atmospheres.

Keywords: exoplanet, super-Earth, organic aerosol, haze, atmospheric composition

Japan Geoscience Union Meeting 2014
(28 April - 02 May 2014 at Pacifico YOKOHAMA, Kanagawa, Japan)

PPS21-23 Room:416 Time:April 29 17:00-17:15

Transmission spectrum models of low-mass exoplanet atmospheres with haze: Application to GJ 3470b

KAWASHIMA, Yui[1*] ; IKOMA, Masahiro[1] ; FUKUI, Akihiko[2] ; NARITA, Norio[2]

[1]The University of Tokyo, [2]National Astronomical Observatory of Japan

Since the first exoplanet was discovered in 1995, detection of more than 1000 exoplanets has been reported. Recently, transit observations of an exoplanet have been done at multiple wavelengths. From a decline in apparent stellar brightness due to a planetary transit, we can measure the plantary radius. In addition, observed dependence of the planetary radius on wavelength (which is often called the transimission spectrum) provides the information of absorption and scattering by molecules and small particles such as haze and clouds in the planetary atmosphere. Thus, the composition of the planetary atmosphere can be constrained by comparison between the observational and theoretical transmission spectra. The constraint on atmospheric composition gives an important clue to the origin of the planet.

Our observational group has recently observed transits of two low-mass exoplanets, GJ 3470b and GJ 1214b, at multiple wavelengths. For both planets, the observed transit radii in the optical wavelength region are greater than those in the near-infrared region, inferring the existence of haze in the atmosphere. While the observed transmission spectrum was already analysed theoretically in detail as for GJ 1214b, there are few researches discussing the theoretical spectrum models incorporating the effect of haze systematically for GJ 3470b. In this study, we have modeled theoretical transmission spectra of low-mass exoplanets orbiting close to their host stars. Then, applying the calculated spectrum models to GJ 3470b and GJ 1214b, we discuss the property of the atmospheres of both planets.

In calculating theoretical spectrum models, we have taken into account the vertical distribution of molecular abundances from the chemical equilibrium calculations, in addition to absorption and scattering of the incident radiation from the host star by molecules and haze particles in the planetary atmosphere. We explore the dependences of the atmosphere's metallicity, C/O ratio and water vapor abundances on the transmission spectrum. We also probe the dependences of haze's height, particle sizes and number density. In comparing the observed and theoretical transmission spectra, we have performed the chi-squared analysis to quantify the validity of each atmospheric model.

Keywords: exoplanets, transits, transmission spectrum models, atmospheric composition, haze

Japan Geoscience Union Meeting 2014
(28 April - 02 May 2014 at Pacifico YOKOHAMA, Kanagawa, Japan)

PPS21-24 Room:416 Time:April 29 17:15-17:30

The SEEDS Exoplanet and Circumstellar Diks Survey

KUZUHARA, Masayuki[1*] ; TAMURA, Motohide[2] ; KUDO, Tomoyuki[3] ; HASHIMOTO, Jun[4] ; KUSAKABE, Nobuhiko[5] ; MATSUO, Taro[6] ; MCELWAIN, Michael[7] ; JANSON, Markus[8] ; TAKAHASI, Yasuhiro[2]

[1]Department of Earth and Planetary Sciences, Tokyo Institute of Technology, [2]Department of Astronomy, The University of Tokyo, [3]Subaru Telescope, [4]H. L. Dodge Department of Physics and Astronomy, University of Oklahoma, [5]National Astronomical Observatory of Japan, [6]Department of Astronomy, Kyoto University, [7]NASA Goddard Space Flight Center, [8]Astrophysics Research Centre, Queen's University Belfas

About 1,000 extrasolar planets (or exoplanets) have been discovered by now. Furthermore, Kepler survey has reported the presences of more than 3,000 exoplanet candidates (Huber et al. 2013). Thus, the planetary systems are common in our Galaxy, but it has known that those exoplanets have a variety of properties. Meanwhile, studies for circumstellar disks, which are the birth-places of planets, have also progressed. In particular, the radio telescope ALMA, whose operations have recently started, have provided intriguing data for the structure properties of protoplanetary disks (e.g., van der Marel et al. 2013; Casassus 2013). ALMA should provide a deep insight to the studies of circumstellar disks.

Direct imaging observations enable the discovery and study of exoplanets orbiting their host stars at wide orbital separations comparable to a few tens of AU, but the detections of those are impractical with indirect techniques such as radial velocity or transit method. Direct imaging is also useful to characterize circumstellar disks. The high-resolution observations of scattered light from protoplanetary disks or debris-disks have provided many important clues to reveal the physical disk-planet connections. We have progressed the SEEDS project, which aims at detecting and characterizing giant exoplanets and circumstellar disks with the Subaru 8-m ground-based telescope, state-or-the-art adaptive optics AO188, and a high-sensitivity infrared camera HiCIAO that we have newly developed. The total SEEDS sample will reach 500 targets, and this target sample adequately covers stellar ages ranging from 1 to 1000 Myr for solar-type stars. Also, intermediate-mass or low-mass stars are included in our SEEDS sample. The survey is currently in its fifth year, and to date, it has identified intriguing structures, such as gaps or spirals, in more than 10 transitional or debris disks (e.g., Hashimoto et al. 2012; Grady et al. 2013). Furthermore, SEEDS has discovered a massive giant planet candidate orbiting the B-type star Kappa Andromedae (Carson et al. 2013) and a Jovian planet in orbit with a size of about 44 AU (GJ 504b) around the G0-type Sun-like star GJ 504. GJ 504b has an estimated mass of about 4 Jupiter masses and effective temperature of 500 K. Among such the wide-orbit exoplanets directly imaged so far, GJ 504b represents the lowest-mass Jovian planet, and the inferred effective temperature is the coldest. The follow-up observations for GJ 504b have revealed the presences of methane in its atmosphere (Janson et al. 2013), allowing us to report the first methane detection in an atmospheres of directly imaged exoplanet. Thus, SEEDS has successfully identified and studied the exoplanets with the previously unknown properties. After the end of SEEDS survey, the comprehensive and statistical analysis of entire survey sample will be carried out. This analysis leads to improve our understanding about exoplanets and circumstellar disks. In addition, it should become a promising clue that connects to future exoplanet/disk studies, such as a survey of extrasolar Earths.

Here, we report the latest achievements of SEEDS project, such as the detection of GJ 504b. Moreover, its whole survey status and progress are also reported, as well as the future plan of SEEDS project.

Keywords: extrasolar planet, debris disk, protoplanetary disk, giant planet, direct imaging observation

Japan Geoscience Union Meeting 2014
(28 April - 02 May 2014 at Pacifico YOKOHAMA, Kanagawa, Japan)

PPS21-P01 Room:Poster Time:April 29 18:15-19:30

Sonic Boom Analysis of Meteorite at Hypersonic Speeds in Earth Atmosphere

YAMASHITA, Rei[1*] ; SUZUKI, Kojiro[1]

[1]Graduate School of Frontier Sciences, The University of Tokyo

The sonic boom followed by the passage of shock waves may cause serious damage on the ground, when a meteorite falls at hypersonic speeds as experienced at the Chelyabinsk meteorite event in February 2013. Therefore, it is important to evaluate the sonic boom generated by the meteorite. In this study, the prediction method of the sonic boom developed in the aeronautical engineering is applied to the case of the meteorite. The nature of the sonic boom propagation in the earth atmosphere is evaluated by the whole-domain simulation technique, which is based on the computational fluid dynamics in the domain bounded by the flying object and the ground (R. Yamashita and K. Suzuki, APISAT2013, No. 02-05-3). The flowfield around the sphere with 20 m diameter is numerically obtained by solving the three dimensional Navier-Stokes equations with the gravity term. The earth ' s atmospheric model is based on the international standard atmosphere (ISO 2533:1975). The flight Mach number is 10 (about 3 km/s), the flight altitude is 10 km and the flight condition is the steady level flight. The computational grid is constructed by rotating the two dimensional grid about the body axis and the number of the grid points is about 5.5 million. After the numerical calculation is conducted by using the initial grid, the calculation is performed again with the adaptive grid reconstructed to align the bow shock wave to avoid the artificial smearing of the shock wave. For computational efficiency, the domain is divided into several sectors from the body to the ground. The shape of the meteorite is approximated as a sphere and the axi-symmetric flowfield is assumed in the sector near the body. The numerical fluxes are evaluated by SHUS scheme (E. Shima and T. Jounouchi, NAL SP, pp.7-12, 1997) with the third order accuracy by MUSCL interpolation technique. The time integration is conducted by MFGS (E. Shima, proceedings of 29th Fluid Dynamic Conference, pp.325-328, 1997) method. The gravity term is added to the governing equations as a source term.

The flowfield around the sphere is composed of the bow shock wave in front of the body and the trailing shock wave in the wake. Both the waves propagating downward are merged into a single wave at 8 km altitude. In such case, the sonic boom sounds only once, while the sonic boom generated by a supersonic airplane creates explosive sounds twice without merging of the shock waves. It is reported that Chelyabinsk meteorite has been broken into three big pieces and the sonic boom sounds three times at the ground (NHK COSMIC FRONT, June 2013). Hence, the number of the pieces is equal to that of the sound of explosion. This fact seems consistent with the present simulation result. The pressure rise across the shock wave decreases with the distance from the body because of the geometric spreading. In the actual earth's atmosphere, however, the rate of decrease becomes smaller near the ground, because the atmospheric pressure and temperature increase toward the ground. Assuming the pressure augmentation factor of 1.9 at the reflection of the shock wave at the ground, the peak pressure rise is estimated at about 1.5 kPa, which is 63 times as large as the maximum allowable pressure rise (24 Pa) determined in the environmental regulation for the supersonic airplane. In the case of the Chelyabinsk meteorite, the pressure rise is estimated at 3.2±0.6 kPa (Nature 12741) from the observation of the damage of the glass windows there. Although the numerical condition is not the same as the actual flight condition of the meteorite, the pressure rise due to the passage of a meteorite at hypersonic speeds is expected to be in the order of 1 kPa or higher.

As mentioned above, the prediction method developed in the aeronautical engineering has a great potential to predict the flight condition, say, the size, altitude and Mach number, from the magnitude of the sonic boom measured on the ground by conducting the parametrical study.

Keywords: Sonic Boom, Meteorite, Hypersonic Flow, CFD, Shock Wave

Japan Geoscience Union Meeting 2014
(28 April - 02 May 2014 at Pacifico YOKOHAMA, Kanagawa, Japan)

PPS21-P02 Room:Poster Time:April 29 18:15-19:30

The brightness and the color temperature of the Chelyabinsk bolide

YANAGISAWA, Masahisa[1*]

[1]Univ. Electro-Communications

The bolide explosion on Feb. 15, 2013 over Chelyabinsk, Russia was the next most violent to the probable bolide explosion in Tunguska, Siberia in 1908. It was recorded by many dashboard movie cameras in a wide area around the city, and the movies are released on the Internet. We analyzed one of them and obtained the lightcurves of the bolide for three colors (see the figure for the temporal variations of the brightness). More than 95% of the radiant energy in the visible wavelengths was released in its flare-up for about 2 seconds. The luminosity ratios among the R (red), G (green), and B (blue) color bands are consistent with the 3500 K black-body radiation during the flare, while the pre-flare bolide was greenish-blue in color and the ratios do not agree to the black-body spectra. The maximum luminosity was 1.0 x 10^{15} W. The impact energy is estimated to be 1.9 x 10^{15} J or 450 kton in TNT equivalent (1 kton = 4.185 x 10^{12} J), based on an empirical formula for the radiant efficiency of bolides. The lightcurves and the impact energy almost agree to the results reported thus far.

Figure caption: Temporal variations of the source luminosities of the bolide in logarithmic scales. The thick (red), dotted (green), and thin (blue) lines correspond to the RGB color bands. The calculated intensities are negative in the periods without plot. The vertical scale on the right side shows the luminosity integrated over the wavelengths assuming 3500 K black body radiation. Seconds of 3:20 on Feb. 15, 2013 (UT) are shown in abscissa.

Keywords: bolide, meteoroid impact, small solar system objects, Chelyabinsk, Space guard, meteorites

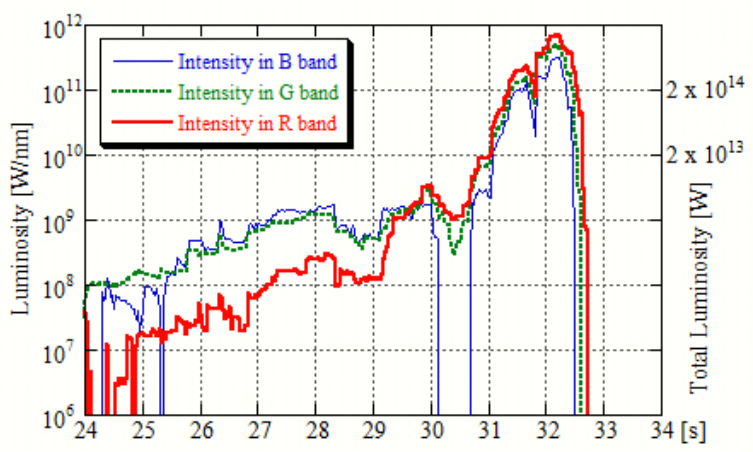

Japan Geoscience Union Meeting 2014
(28 April - 02 May 2014 at Pacifico YOKOHAMA, Kanagawa, Japan)

PPS21-P03 Room:Poster Time:April 29 18:15-19:30

Statistical distribution of the solar system dusts by meteor head echo observations with the large-aperture radar

ABE, Shinsuke[1*] ; KERO, Johan[2] ; NAKAMURA, Takuji[3] ; FUJIWARA, Yasunori[4] ; WATANABE, Jun-ichi[5]

[1]Department of Aerospace Engineering, College of Science and Technology, Nihon University, [2]Swedish Institute of Space Physics (IRF), [3]National Institute of Polar Research (NIPR), [4]Nippon Meteor Society, [5]National Astronomical Observatory of Japan

A meteor head echoes is caused by radio waves scattered from the intense region of the plasma surrounding and co-moving with a meteoroid during atmospheric entry at about 70-130 km altitude. Meteor head echo observations were carried out using the high-power large-aperture (HPLA) Kyoto university Shigaraki middle and upper atmosphere (MU) radar in Japan (34.85deg N, 136.10deg E). Since 2009 the atmospheric trajectories and interplanetary orbital elements have been derived by the MU radar meteor head echoes (e.g.; Kero et al. (2012); Kero et al. (2011)). Approximately 120,000 orbital elements of meteors with excellent accuracy were obtained until January 2014. Typical error for velocity and semi-major axis are 0.3 km/s and 0.1 AU, respectively. Such a huge number of meteoroid orbits with the precise orbital accuracy has not been observed before. Here we report some results obtained by the statistical analysis of the database, such as orbital distributions and associations of comets and asteroids.

Keywords: meteors, dusts, meteoroids, comets, asteroids, MU radar

Japan Geoscience Union Meeting 2014
(28 April - 02 May 2014 at Pacifico YOKOHAMA, Kanagawa, Japan)

PPS21-P04 Room:Poster Time:April 29 18:15-19:30

Laboratory experiment simulating Martian surface observation with submillimeter-wave polarimetric radiometry

ARIMURA, Taketo[1*] ; OCHIAI, Satoshi[2] ; KIKUCHI, Kenichi[2] ; KITA, Kazuyuki[3] ; KASAI, Yasuko[2]

[1]Graduate School of Science and Engineering, Ibaraki University, [2]National Institute of Information and Communications Technology, [3]Faculty of Science, Ibaraki University

Energies and materials exchange between the ground and atmosphere on Mars play important roles in the Martian general circulation. It is necessary to observe the spatial and temporal variability of the Martian surface from orbiter. However, it has been quite difficult to continually monitor the Mars surface in optical observation due to opaqueness of the Martian dust. Millimeter/submillimeter radiometers enable to observe the Martian surface through dust, though such measurement has never been conducted in planetary exploration. We assess the effectiveness of this observation method by laboratory experiment.

By observing millimeter/submillimeter emission from the Martian surface in several emission angles and two polarizations, we can derive physical temperatures, permittivity and roughness of the surface from brightness temperatures. In order to estimate each property from polarized brightness temperatures, we need to know relationship between emissivity or/and reflectivity in millimeter/submillimeter wave region and the parameters of surface.

We developed an experiment system to examine millimeter/submillimeter scattering and emission characteristics of the simulated Martian surface in a chamber. Measurement samples in the chamber are coolable at Martian surface temperature. The chamber is designed to measure emission of samples using a receiver and reflection of samples using a transmitter and a receiver. We can also obtain arbitrary-polarized emission with arbitrary incident angle by controlling mirrors in our system.

To discuss relationship between emission and surface parameters on the Martian surface, it is necessary to know influences of permittivity and surface roughness on the reflectivity. Therefore, we measured reflectance of Acrylic plate and Alumina grain at millimeter/submillimeter waves region. We discuss effects of permittivity and roughness on measured reflectivity of measurement samples in known polarization and incident angle. Moreover, we retrieve the permittivity and the roughness of sample from measured reflectivity. Using this measurement results, we expect a step closer to explanation of relationship between emission and surface parameters in the Martian surface at millimeter/submillimeter waves region.

Keywords: Mars, surface observation, submillimeter-wave

Japan Geoscience Union Meeting 2014
(28 April - 02 May 2014 at Pacifico YOKOHAMA, Kanagawa, Japan)

PPS21-P05 Room:Poster Time:April 29 18:15-19:30

Scientific importance and possibility of HCN detection in Enceladus plumes by ALMA

KODAMA, Kenya[1*] ; SEKINE, Yasuhito[1] ; IINO, Takahiro[2] ; SAIGO, Kazuya[6] ; KASAI, Yasuko[3] ; SAGAWA, Hideo[4] ; MAEZAWA, Hiroyuki[5]

[1]Dept. Complexity Sci. and Engr. Univ. of Tokyo, [2]Solar-Terrestrial Environment Laboratory,Graduate school of science,Nagoya University, [3]Senior Researcher Global Environment Division National Institute of Information and Communications, [4]National Institute of Information and Communications Technology, [5]Department of Physical Science Osaka Prefecture University, [6]National Astronomical Observatory of Japan

Saturn's icy moon, Enceladus, exhibits ongoing geological activities, including eruption of water-rich plumes from warm fractures near the south-pole region. These geological activities together with the findings of Na-rich salts in the plumes suggest the presence of an interior liquid ocean beneath the icy crust. This demonstrates that Enceladus' plumes provide a unique opportunity to investigate the chemical composition of oceanic water, possible geochemical reactions, and habitability of the icy moon. However, due to limitations of in-situ measurements of the plumes by the Cassini spacecraft, it is not able to identify or quantify some key molecules, which could probe physical and chemical conditions of the ocean.

Here we discuss scientific importance and possibility of detection of HCN in the plumes by large ground-based, sub-millimeter telescope, ALMA. Because HCN is one of the fundamental materials contained in icy planetasimals in the outer solar system, and because it readily hydrolyzes in warm water($>$50 ℃), a lack of HCN suggests that Enceladus' interior would have experienced relatively high temperatures, i.e., a presence of hydrothermal activity. On the other hand, if HCN were presence in the plumes, this in turn means that Enceladus would have been cold throughout its history. Given the results of thermal evolution model, the latter case suggests late formation of the Saturnian system($>$5Myr) after CAI formation, which would result in a depletion of short-lived radiogenic heat source in Enceladus.

To evaluate the possibility to detect HCN in the plumes by ALMA, we first estimate a special distribution of H_2O gas density based on results from Cassini's observations and plume eruption modeling. Then, we calculate radiactive temperatures of HCN in the field of view of ALMA as a function of HCN concentration. Finally, the upper limit of HCN as a function of observation time will be obtained. For instance, if HCN were not detected within 4-6 hours of observation time, an upper limit of the HCN concentration in the plumes becomes 0.2% relative to water, which is comparable to a typical concentration of HCN in comets. Thus, the ALMA telescope is capable of detecting HCN in Enceladus' plumes within a reasonable observation time, if it were present in an amount comparable to that of comets. In either case whether HCN were presence or not, we would be able to constrain geochemical reactions and thermal history of Enceladus as well as the timing of formation of Saturnian system.

Japan Geoscience Union Meeting 2014
(28 April - 02 May 2014 at Pacifico YOKOHAMA, Kanagawa, Japan)

PPS21-P06 Room:Poster Time:April 29 18:15-19:30

Development of SPH: Toward Understanding of Disk-planet Interaction Near the Disk Inner Edge

FUJII, Yuri[1*] ; IWASAKI, Kazunari[1] ; TSUKAMOTO, Yusuke[1] ; INUTSUKA, Shu-ichiro[1]

[1]Nagoya University

Recent observations of exoplanets reveal the existence of close-in planets. These planets are thought to form in outer disks and migrate inward because of the disk-planet interaction. If there are disk inner cavities, planets can stop migrating and stay in close-in orbit. Disk evolution is highly affected by these planets. Thus, the understanding of the interaction between disks and close-in planets is crucial. In this study, we develop a numerical scheme to investigate the interaction between disks and planets. Although the grid-based schemes are widely used in this context, there are difficulties in calculating with a disk inner cavity or eccentric planets. These difficulties can be removed by smoothed particle hydrodynamics (SPH) with high accuracy. In this presentation, we will talk about the development of code and the performance evaluation.

Keywords: exoplanet, protoplanetary disk, smoothed particle hydrodynamics

Japan Geoscience Union Meeting 2014
(28 April - 02 May 2014 at Pacifico YOKOHAMA, Kanagawa, Japan)

PPS21-P07 Room:Poster Time:April 29 18:15-19:30

Evolution of a protoplanetary disk and chemical composition of planetesimals

NAGAHARA, Hiroko[1*] ; OZAWA, Kazuhito[1]

[1]Dept. Earth Planet. Sci., The Univ. Tokyo

We investigate physico-chemical evolution of the proto-solar disk at the early stage by developing a new model that combines physics and chemistry with special interest to temporal and spatial evolution of the disk. Then, we discuss how the composition of planetesimals varies depending on the time and space for their formation including refractory or volatile rich ones.

The basic of the model is a radial advection-diffusion equation, which includes drift and dispersion by turbulence with stochastic diffusion term calculated by the Monte Carlo method and which shows the diffusivity by the viscosity of the disk. The difference from conventional disk models is that the present method stands on the Lagrangean differentiation, and it is able to trace the movement of individ- ual particles.

A considerable amount of materials in the inner regions are transported outward at the early stage (t <10^5 yrs), which is because the surface density is much larger in the inner region at the early stage of the disk evolution. Although the outward flux is large at the early stage, there comes a larger amount of materials from the outer region even within ~10^5 yrs. The mixing ratio of materials from the inner regions to outer regions is almost unity within several AU all through the disk evolution, suggesting that thermally processed materials and unprocessed materials were mixed in the inner region of the disk. It is important that the relative abundance of materials from outer regions becomes larger with time, which implies that planetesimals formed within several AU at the early stage of the disk evolution consists partly of materials initially located at the inner regions and partly from outer regions, but those formed at the later stage contain more abundant law materials transported from the outer regions.

The mixing ratio of materials from the inner and outer regions is almost unity at the early stage but the fraction of materials from the outer regions increases with time. Combining the information about the maximum temperature that the particles experienced, we can constrain that early differentiated planetesimals such as the parent body of angrites and planetesimals with refractory-rich compositions such as CV chondrites were formed at the inner region of the disk in ~10^5 yrs. On the other hand, planetesimals for other carbonaceous chondrites or ordinary chondrites that are depleted in sulfur were formed later, possibly at ~10^6 yrs.

Keywords: protoplanetary dsik, chemical evolution, dust movement

Japan Geoscience Union Meeting 2014
(28 April - 02 May 2014 at Pacifico YOKOHAMA, Kanagawa, Japan)

PPS21-P08 Room:Poster Time:April 29 18:15-19:30

Simulating global dust coagulation with grain charging

OKUZUMI, Satoshi[1*] ; TANAKA, Hidekazu[2]

[1]Graduate School of Science and Engineering, Tokyo Institute of Technology, [2]Institute of Low Temperature Science, Hokkaido University

Growth of dust particles by collisions is the initial step of planet formation. Conventionally, the theory of dust coagulation in protoplanetary disks assumed electrically neutral dust particles, but in reality dust in the disks is likely to be charged given that the disks are ionized by cosmic rays and stellar X-rays. In our previous work (Okuzumi 2009; Okuzumi et al. 2011a,b), we extensively studied the role of grain charging in protoplanetary dust growth, and concluded that dust growth stalls at its early stage because of the excessively large (negative) charges carried by small dust aggregates. We also predicted that this ”charge barrier” could be overcome (albeit on a very long timescale) if dust in the disks is globally transported by radial drift and turbulent diffusion.

The purpose of the present work is to demonstrate the breakthrough of the charge barrier in a global setup. In order to do this, we have developed a new simulation code for global dust coagulation including the effect of grain charging. The new code is based on a previous code for planetesimal formation (Brauer et al. 2008; Okuzumi et al. 2012) but now calculates charging and Coulomb repulsion of dust particles at each location in a disk consistently with the particle size distribution at the same location. To verify the code, we perform some test simulations and compare them with the prediction from our previous theory.

Keywords: dust, charging, planet formation, protoplanetary disk

Japan Geoscience Union Meeting 2014
(28 April - 02 May 2014 at Pacifico YOKOHAMA, Kanagawa, Japan)

PPS21-P09 Room:Poster Time:April 29 18:15-19:30

N-body simulations of Rubble pile Collisions in Tidal fields

HYODO, Ryuki[1*] ; OHTSUKI, Keiji[1]

[1]Kobe University, Graduate School of Science

We examine collisional disruption of gravitational aggregates in the tidal environment by using local N-body simulations. We find that outcomes of such collision largely depend on impact velocity, direction of impact, and radial distance from the planet. In the case of a strong tidal field corresponding to Saturn's F ring, collisions in the azimuthal direction is much more destructive than those in the radial direction. Numerical results of collisions sensitively depend on impact velocity, and complete disruption of aggregates can occur even in impacts with velocity much lower than their escape velocity. In such low-velocity collisions, deformation of colliding aggregates plays an essential role in determining collision outcomes, because the physical size of the aggregate is comparable to its Hill radius. On the other hand, the dependence of collision outcomes on impact velocity becomes similar to the case in free space when the distance from the planet is sufficiently large. We submitted the results to the Astrophysical Journal.

Keywords: rings, satellites, aggregates

Japan Geoscience Union Meeting 2014
(28 April - 02 May 2014 at Pacifico YOKOHAMA, Kanagawa, Japan)

PPS21-P10 Room:Poster Time:April 29 18:15-19:30

An improved fragmentation model on outcome of planetesimal collisions

FUJITA, Tomoaki[1] ; GENDA, Hidenori[2*] ; KOBAYASHI, Hiroshi[3] ; TANAKA, Hidekazu[4] ; ABE, Yutaka[1]

[1]Department of Earth and Planetary Science, University of Tokyo, [2]Earth-Life Sicence Institute, Tokyo Institute of Technology, [3]Department of Physics, Nagoya University, [4]Institute of Low Temperature Science, Hokkaido University

Collisions between planetesimals or a planetesimal and a protoplanet are thought to occur frequently in the stage of planet formation, and these planetary bodies grow up through these collisions. However, if destructive collisions between them occur frequently, these bodies break up into fragments rather than promote the growth of them. Therefore, in order to understand the process of the growth for planetesimals and protoplanets, it is important to know the impact conditions under which a collision is destructive. The critical specific impact energy for catastrophic disruption $Q_D{}^*$, where the largest remnant has half the target mass, has been well investigated under various conditions so far (Holsapple et al., 2002; Benz & Asphaug, 1999; Leinhardt & Stewart, 2009). Such catastrophic impacts have been regarded as important process for planet formation. The values of $Q_D{}^*$ which has been referred and used most frequently were calculated by Benz and Asphaug (1999). Although they performed many impact simulations to determine $Q_D{}^*$, the resolution of their numerical simulation were quite low and they did not check the resolution convergence of $Q_D{}^*$. In addition, recent studies (Kobayashi & Tanaka, 2010; Kobayashi et al., 2010) have suggested that non-disruptive small-scaled impacts were also important to the growth of protoplanets, because these small-scaled impacts are much more frequent than disruptive impacts.

In order to discuss more correctly the growth of planets, a correct value of $Q_D{}^*$ and the relation between ejecta mass and impact energy for small-scaled impacts should be required. In this thesis, I investigate the resolution dependence of $Q_D{}^*$ and obtain a correct value of $Q_D{}^*$ for planetesimal collisions by numerical impact simulations with sufficient resolution. I also investigate small-scaled impacts, and formulate the relation between the ejecta mass and impact energy.

Using the smoothed particle hydrodynamics method (SPH) with self-gravity and without strength, I systematically perform the hydrodynamic simulations of collisions between rocky planetesimals. I consider collisions of 10 km and 100 km rocky targets and various sized impactors under various conditions such as impact velocity, impact angle and resolution.

I found that the value of $Q_D{}^*$ depended on resolution. This is because distribution ratio of initial impact energy to kinetic and internal energy of a target differs depending on resolution due to shear flows which appears during propagation of shock wave and rarefaction wave and ejection process. This energy distribution ratio, probably also $Q_D{}^*$, converges in using 7.5×10^7 particles. The resolution in Benz & Asphaug (1999), where they performed impact simulations with 5×10^4 particles, was insufficient. The $Q_D{}^*$ obtained by higher-resolution simulations is about a half order of magnitude smaller than that of Benz and Asphaug (1999). This means collisions between planetesimals or a planetesimal and a protoplanet are more destructive than previously thought. I applied improved $Q_D{}^*$ to the growth of protoplanets using analytical method proposed by Kobayashi et al. (2010). As a result, the mass of the finally formed protoplanet is a half smaller than the case for previous $Q_D{}^*$. In addition, I derived the formulation of scaling law representing the relation between ejecta mass and impact energy from small-scaled impacts to destructive impacts. I found that this relation can be scaled by target size, impact energy normalized by $Q_D{}^*$, and impact velocity, but it depend on impact angle. With $Q_D{}^*$ and the scaling law obtained in this study, the final grown mass of a protoplanet is 0.058 M_{earth} at 1AU and 0.17M_{earth} at 5 AU, where M_{earth} represents the Earth mass.

Japan Geoscience Union Meeting 2014
(28 April - 02 May 2014 at Pacifico YOKOHAMA, Kanagawa, Japan)

PPS21-P11 Room:Poster Time:April 29 18:15-19:30

Numerical modeling of impact phenomena using iSALE shock physics code

KUROSAWA, Kosuke[1*] ; SENSHU, Hiroki[1] ; WADA, Koji[1] ; MIKAMI, Takashi[2] ; HIRATA, Naru[3] ; KAMATA, Shunichi[2] ; ISHIHARA, Yoshiaki[4] ; GENDA, Hidenori[5] ; NAKAMURA, Akiko[6] ; TAKATA, Toshiko[7]

[1]PERC, Chitech, [2]Dept. of CosmoSciences, Hokkaido Univ., [3]Dept. of Computer Sci. & Eng., The University of Aizu, [4]ISAS, JAXA, [5]ELSI, Titech, [6]Dept. of Earth and Planetary Sciences, Kobe University, [7]Division of Science Education, Miyagi University of Education

iSALE (impact-SALE) is a shock physics code based on the SALE hydrocode (Simplified Arbitrary Lagrangian Eulerian), which is an open code for planetary scientist. iSALE contains a number of option to model impact phenomena of geological materials. The calculation results can be easily visualized and analyzed using included software. A number of ANEOS tables and strength models of geological materials, including water ice, silicate rocks, and iron are also included. We have formed a user community called " iSALE users group in Japan " to introduce iSALE to the Japanese society for planetary science and to share information on the usage of iSALE. The URL of our wiki page and the mailing list are as follows.

The URL of the wiki page of iSALE users group in Japan
https://www.wakusei.jp/~impact/wiki/iSALE/

Mailing list
isale-users-jp@perc.it-chiba.ac.jp

In the presentation, we show the results of a number of test calculations using iSALE.

We gratefully acknowledge the developers of iSALE, including Gareth Collins, Kai W$\bar{u}$
nnemann, Boris Ivanov, Jay Melosh and Dirk Elbeshausen.

Keywords: Hypervelocity impacts, Shock physics code, Hydrocode calculation, Equations of state, strength model, iSALE

Japan Geoscience Union Meeting 2014
(28 April - 02 May 2014 at Pacifico YOKOHAMA, Kanagawa, Japan)

PPS21-P12 Room:Poster Time:April 29 18:15-19:30

Study on fundamental characteristics of penetration dynamics into icy target

NAMBA, Kazuya[1*] ; SUZUKI, Kojiro[2]

[1]Grad. Sch. Eng., The University of Tokyo, [2]GSFS, The University of Tokyo

A penetrator, which penetrates the surface of a planet, a satellite and so on to investigate the interior by high-speed hard landing, is expected to play an important role in the solar system exploration of the future. Comparing to soft lander, penetrator has advantages of consuming less fuels, enabling us to launch multiple probes at a time because of its low mass, and so on. However, probe must survive hard impact in collision, thus no penetrator missions have been successfully achieved so far. The icy object, such as 24 Themis and Europa, is expected to contain organics which serve as the precursor of life in their subsurface. Therefore, the cryo-penetrator, which penetrates the icy object and investigate specimens of subsurface which have not been contaminated by cosmic rays, should have a high importance. For a penetrator into regolith, a fully-developed flyable penetrator has been successfully developed for the Lunar-A mission, though the mission itself has been cancelled. For icy target, however, the number of studies from the engineering viewpoint is quite limited, for example, the conceptual study on CRAF mission to a comet nucleus (Adams et al., NASA CR-177393, 1986). In this study, we investigated the fundamental properties of the penetration dynamics of the cryo-penetrator, by conducting penetration experiments into the target made from H_2O ice.

Penetration experiments were conducted by using a ballistic range in our laboratory. The projectile is accelerated by the compressed air, launched horizontally and crashed into a target body. Impact speed is set from 100 m/s to 300 m/s. Two types of projectile, a needle-like one (iron, size: ϕ2.45x15mm, mass: 1.71g) and a blunt cone-like one (brass, ϕ8.4x15mm, 2.33g) are used. Three types of target, pure H_2O ice (size: 270x175x130mm, mass: 5.5kg, density: 0.90g/cm^3, porosity: 3%), low purity H_2O ice (150x120x100mm, 1.5kg, 0.75g/cm^3, 19%) and an oil clay (155x120x70mm, 2.2kg, 1.7g/cm^3) are used. A high-speed camera (frame rate: 2200-8800fps, exposure time: 15μs) is used to observe a sequence of events: the free-flight of the projectile, impact, crater formation, penetration, and so on.

We found that the penetration into H_2O ice produces ejecta of icy fragments, which erupt conically immediately after collision, and then produces the jet-like ejecta in the almost perpendicular direction to the surface that continues more than 100 msec. On the other hand, the penetration into clay target produces ejecta outward-conically for duration of a few msec. Moreover, we found that the penetrator tends to be pushed back from the target by the ejecta, since the ice around the projectile has been almost broken into pieces erupting as the ejecta and the penetrator cannot be fixed inside the target without receiving the gripping force from the ice. We also found that eruption was continued even after the projectile has completely bounced from the target. This phenomena is frequently observed when the projectile with a less slender body. In the case of a slender penetrator, however, it is hardly subject to bounce-back. Consequently, a slender shape seems more suitable to the penetrator for icy target. The shape of crater consists of the pit region on the center, the spall region which is a shallow depression on the periphery of the pit, and cracks spread a wide range of target. It is qualitatively consistent with previous researches using bullet shape (e.g. Kato et al., Icarus 113(2) 423-441, 1995., Arakawa, Low Temperature Science 66 113-121, 2008). The pressure at a point of impact is estimated by using the one-dimensional planar impact approximation (Wada, JSIAM 16(4) 19-31, 2006): the result shows that it is beyond the Hugoniot elastic limit (HEL), thus the H_2O ice is expected to behave like fluid in the vicinity of the impact point.

This work is supported by Grant-in-Aid for Scientific Research (B) No. 25289301 of Japan Society for the Promotion of Science.

Keywords: icy object, penetrator, crater, ballistic range

Japan Geoscience Union Meeting 2014
(28 April - 02 May 2014 at Pacifico YOKOHAMA, Kanagawa, Japan)

PPS21-P13 Room:Poster Time:April 29 18:15-19:30

Experimental study of compaction process of powder bed by centrifuge experiment

OMURA, Tomomi[1*] ; KIUCHI, Masato[1] ; GUETTLER, Carsten[2] ; NAKAMURA, Akiko[1]

[1]Graduate School of Science, Kobe University, [2]Max-Planck-Institute for Solar System Research

Dust aggregates in protoplanetary disk are compacted by dust-dust collisions, ram pressure of the disk gas and self-gravity (Kataoka et al., 2013). At reaccumulation phase of asteroids, porosity of rubble pile and regolith would be determined by collisional pressure and self-gravity.

Relationship of porosity of powder layer and particle's radius is given by (Yu et al., 2003; Kiuchi and Nakamura, 2014)

$p=p_0+(1-p_0)\exp\{-mR_F^{-n}\}$ (1)

where R_F is the ratio between the magnitudes of the van der Waals force between two particles and gravity force on particles, therefore a function of particle radius. p_0, m, and n are constants. p_0 should be understood as the porosity without any interparticle force.

It is not clear if Eq.1 can be applied for powder layer under different gravity from 1 G. Eq.1 was originally derived for particles at surface, and we don't know to what extent this equation is able to be applied for the interior of planetary bodies, i.e., it has not examined for the porosity evolution of bodies due to the accumulation of new grains and blocks onto the surface. If Eq.1 is applicable to such case, porosity given by Eq.1 should be consistent with the result of the case in which R_F is reduced by increasing the gravity. In this study we perform experiments, under different gravitational accelerations, and we compare the results with Eq.1.

We use silica sand, 60 wt% of grains have sizes ranging from 7.5 μm and 80 μm and fly ash, 60 wt% of grains have sizes ranging from 1 μm and 8 μm. They were sieved into a cylindrical container of diameter 5.8 cm and depth 3 cm. After that, the top part of the bed over the height of the container was leveled off. Porosity of each granular bed is approximately 60 % and 70 %. The experiments were performed at elevated acceleration on a centrifuge to provide 1-18 G and observed with a video camera. In contrast with unidirectional compressive compaction using a piston, centrifugal compaction is capable of applying uniform compressive force at any place of the container without causing any local disturbance (Mizuno et al., 1991). After the materials were compressed, bed height was measured with a laser displacement meter and the difference between the initial bed height and the average bed height after acceleration was calculated.

As a result, it is shown that Eq.1 is consistent with experimental result within 6 % (silica sand) and 5% (fly ash) in porosity when assuming the grain diameter=24 μm and 4.5 μm, respectively. This diameter corresponds to the median of cumulative weight distribution of the grains. Also, the diameter of the small silica sand grains sticked with large grains is close to 24 μm.

Keywords: planetesimal, asteroid, porosity, high gravity, powder and granular material

Japan Geoscience Union Meeting 2014
(28 April - 02 May 2014 at Pacifico YOKOHAMA, Kanagawa, Japan)

PPS21-P14 Room:Poster Time:April 29 18:15-19:30

High velocity impact cratering experiments on ice-sand mixture simulating the surface of icy satellites

TAKANO, Shota[1*] ; ARAKAWA, Masahiko[1] ; YASUI, Minami[2]

[1]Graduate School of Science, Kobe University, [2]Organization of Advanced Science and Technology, Kobe University

It is well known that ice-rock mixtures could be a main component of icy satellites, the surface crust of asteroid Ceres. Ceres' icy crust could be impacted by various asteroids with different components and physical properties will affect the crater morphology. Therefore, we would obtain various information from the investigation of the observed craters such as material properties of impacted asteroids and the internal structures of the icy crust and so on. To conduct these investigation, the laboratory experiments would be necessary to derive such information from the observed crater. Then, we should carry out the cratering experiments on ice, ice-rock mixtures and the layered target.

Impact experiments on ice has been conducted systematically under various conditions. However, the cratering experiments on ice-rock mixture were limited in the impact velocity range and the rock contents. It is necessary to experiment at the velocity higher than 4km/s to apply to craters on Ceres, but it is not done now. Therefore, we made cratering experiments on ice?rock mixtures at the impact velocity higher than 1km/s using the several types of the projectile, and compared them with the pure ice to clarify the effects of rock inclusion on the crater morphology and crater scaling law.

We installed and used a new two-stage light gas gun at Kobe University in 2013. We prepared ice-rock mixture targets simulating Ceres crust which consisted of water ice and quartz sand having a particle size of about 500μm, and the quartz content was regulated to be 81$\pm$2wt%. The ice-sand mixture was made in a cylindrical metal container with the height of 5$\sim$10cm and the diameter of 15cm. The water-sand mixture was frozen in a freezer with the temperature from -23 ℃ to -15 ℃. Used spherical projectiles were made of aluminum (2.7g/cm3), titanium (5g/cm3), and zirconium (5.7g/cm3), respectively. We lunched projectiles at 1.6$\sim$5.1km/s with nylon sabots to use various types of projectiles. To prevent targets from melting, the vacuum chamber was evacuated for insulation. The chamber pressure during the experiments was from 200 to 230Pa. A crater formation process was taken by an image-converter camera every 5μs, and 18 successive images were obtained for each shot. From these images, we examined the characteristics of impact eject such as the growth rate, and the shape, and it was compared with that of pure ice. We measured the crater shapes by a caliper.

We found that the spallation was difficult to occur on the ice-rock mixture targets compared to pure ice targets. So, the depth-diameter ratio of the crater for ice-rock mixtures, these dependencies on the velocities, and the projectile densities was different from that of pure ice targets. We found that the crater diameter on the ice-rock mixture is about a half of that on pure ice at the same impact energy. Hiraoka et al. (2004) made the cratering experiments on ice-rock mixture with the rock contents from 0 to 50 wt% at the constant impact energy. We compared their results with our results obtained for 80 wt% and found that our result is almost consistent with their results of 50 wt% content. This means that the crater size stop decreasing at 50 wt%, then it becomes almost constant until 80 wt%. We speculate that the crater size might drastically change to be small between 80 to 100 wt% corresponding to rock itself. It might be possible that the crater size could be controlled by the ice strength from 0 to 80wt% and by the rock strength at the range of content near 100 wt%. The crater scaling law proposed by Housen and Holsapple (2012) was applied, and the scaled crater radius π_R and the scaled strengthπ_Y were investigated in our results. Our results were compared with that of pure ice and the ice-rock mixture's dynamic tensile strength was supposed to be 100MPa if the ice-rock mixture was scaled by the same parameter as that of pure ice.

Keywords: icy satellites, ice-sand mixture, impact crater, high velocity impact experiments

Japan Geoscience Union Meeting 2014
(28 April - 02 May 2014 at Pacifico YOKOHAMA, Kanagawa, Japan)

PPS21-P15 Room:Poster Time:April 29 18:15-19:30

Experimental study on the decay process of impact-induced stress propagating through granular materials

MATSUE, Kazuma[1*] ; ARAKAWA, Masahiko[1] ; YASUI, Minami[2]

[1]Graduate School of Science, Kobe University, [2]Organization of Advanced Science and Technology, Kobe University

Introduction: Impact process is one of the most important physical processes in the solar nebula. In order to understand the impact histories related to planetary formation process, it is important to study the impact cratering process and the scaling law. Impact cratering experiments have been performed on granular material, and the crater size is found to be different depending on the target material. So, it is necessary to study how physical properties affect the cratering process, especially for excavation stage. Excavation flow is a main process that controls the crater size, so we should examine the effects of material properties. However, it is difficult to observe the flow inside the target, so we used the in-material sensor to measure the pressure. The pressure distribution in the granular target would show the flow and we can compare the crater size and the pressure distribution to clarify the effect of target materials on the crater formation process.

Experimental method: We prepared a target container with a pressure sensor to measure the stress generated by impact. It is made of aluminum with the size of 10cm×10cm×10cm, and we changed the depth of the granular target from 1 to 10cm. The pressure sensor (20kPa, ≤2kHz)was attached on the bottom of the container just below the impact point, and impact experiments were conducted by a free-fall or by a one-stage vertical He-gas gun in Kobe University. We studied the effects of projectile size and impact velocity on the crater size and the stress wave. We used glass beads and quartz sand with the diameter of 100 and 500μm as granular target, and glass balls (ϕ=7.75, 10, 15mm) in free-fall, nylon and alumina (ϕ= 3mm) in vertical gun experiments as projectile. Impact velocity is 2-5.5m/s in free-fall and 60-70m/s in vertical gun experiments. We observed crater size and pressure wave in each experiment.

Results: We found that the size of the impact crater strongly depends on the granular materials, that is, the crater formed on the quartz sand was systematically smaller than that formed on the glass beads. Then, we found that the pressure wave increased suddenly and decreased with a relaxation time depending on target materials. The relaxation time is small for quartz sand and long for glass beads, and the relaxation time of 100μm quartz sand was not measured because of normal mode oscillation of the pressure sensor: it means that the time is less than 0.5ms.

Although the normal mode oscillation of the sensor was observed in the high velocity impact and the shallow depth impact in the case of gas gun experiments, we analyzed the peak of measure pressure waves (P_{max}) and obtained the relaxation time (τ) by fitting them with the following function: $P(t)$-$P(\infty)$=$A\exp(-t/\tau)$, where t is time after the impact. As a result, τ is obtained to be 1ms for glass beads target irrespective of the bead size, and 0.1ms for 500μm quartz sand. The relationship between the pressure and the propagation distance was described by $P(r)=P_0(r/L)^{-b}$, where L is a projectile radius, r is distance, P_0 is an initial impact pressure, and b is a decay constant. The decay constant was found to change with the impact velocity and the target materials: it was derived to be 0.79,0.94 in a low velocity range, 1.61,1.71 in a high velocity range for glass beads, quartz sand.

We found that the relationship between the crater size and P_{max} at 4cm depth was different in each granular material. The crater size of the glass beads target was larger than that of the quartz sand at the same P_{max} . Then, we introduce a new parameter expressed by τ times P_{max}, so called impulse, I. We renewed the relationship using I instead of P_{max} and found that all data set were merged on one line. This means that I could be a suitable parameter to describe the material dependence of the cratering efficiency. We would like to clarify what material properties determine the τ and how it changed with the physical condition in the future.

Keywords: Excavation flow, Granular material, Cratering process

Japan Geoscience Union Meeting 2014
(28 April - 02 May 2014 at Pacifico YOKOHAMA, Kanagawa, Japan)

PPS21-P16 Room:Poster Time:April 29 18:15-19:30

Effects of impact angles on the impact strength of icy and rocky planetesimals for the collision among equal size bodies

KOMOTO, Yasunari[1] ; ARAKAWA, Masahiko[1] ; YASUI, Minami[2*]

[1]Graduate School of Science, Kobe University, [2]Organization of Advanced Science and Technology, Kobe University

Introduction: There are a lot of impact experiments to simulate planetesimals collisions, and most of them had a large mass difference between a projectile and a target. The impact strength is well known that they are described by the energy density: the ratio of the projectile kinetic energy to the mass of the target and the projectile. So, when the projectile is rather smaller than the target (this is an usual situation in the lab. experiments), the very high speed more than 1 km/s is necessary to disrupt the target. This is an analogy of the present asteroid collisions, but it might be far from the simulation expected in planetesimals collisions. Because we speculate the collisions among the similar size small bodies in the solar nebula, and the relative collisional velocity among them could be several 10 m/s. Therefore, it should be important that the planetesimals were disrupted or not at the impact speed around several 10m/s for the collisions among similar size small bodies, then we must conduct the collisional experiments to derive the impact strength of planetesimals in the similar size collisions. In this study, we carried out the impact experiments using the equal size ball made of ice, gypsum, and gypsum-glass beads mixture. These samples simulate icy planetesimals, planetesimlas for chondrite parent bodies. We also conducted not only head-on collision but also oblique collision and studied the effects of impact angles on the impact disruption.

Experimental methods: We prepared three types of ball sample with the size of 25 mm and 30 mm made of ice, gypsum-glass beads mixture, and gypsum. They were made by putting each solution in a round mold to form spherical sample. The impact experiments were made by using three types of accelerators: they are a spring gun for low velocity collision, a vertical gas gun for ice and a horizontal gas gun for gypsum, and the achieved velocity is from 4 to 160m/s. The oblique impact was also conducted by shifting the impact point from the geometrical center of the target. The impact angle was changed from 0 deg. (normal impact) to 80 deg. (nearly passing away impact). Impact experiments were observed by a high-speed camera and all of the impact fragments were collected to measure the weight and establish the size distribution. We looked for the recovered fragments to identify the same fragment found in the video image, and tried to construct the velocity-mass distribution of the impact fragments.

Results: We used the reduce mass to calculate the impact energy in the center-of-mass system, so the energy density Q_g was defined by the ratio of the kinetic energy of two bodies in the center-of-mass system to the mass of the two equal balls. The impact strength was obtained for the similar size collisions by using this Q_g. As a result, the impact strength ${Q_g}^*$ of ice and gypsum was derived to be almost similar to that obtained for the impact experiments with the mass difference more than 10. However, the ${Q_g}^*$ of glass beads-gypsum mixture was derived to be rather smaller than that obtained in the previous experiments. In the oblique impacts, the mass of the maximum impact fragment was found to decrease with the increase of the impact angle. So, we modify the energy density by using the velocity component normal to the impact surface which effectively work for the disruption, then this modified energy density enabled us to fit all of the data on one line for each target. Finally, we estimated the re-accumulation condition of planetesimals according to the velocity distribution of the impact fragments that obtained in this study. As a result, it is speculated that icy planetesimals could re-accumulate for the bodies larger than 20 km in the diameter, and this threshold size for the planetesimals of ordinary chondrite parent bodies is 5.2km and that for the planetesimals of carbonaceous chondtite parent bodies is 6.7km.

Keywords: Planetesimals, Oblique impact, Impact strength, Energy partition, Re-accretion

Japan Geoscience Union Meeting 2014
(28 April - 02 May 2014 at Pacifico YOKOHAMA, Kanagawa, Japan)

PPS21-P17 Room:Poster Time:April 29 18:15-19:30

Dynamic compaction experiments of porous materials: Implications for impact compaction of pre-planetesimals

YASUI, Minami[1*] ; YOKOTA, Mizuki[2] ; SAKAMOTO, Kana[2] ; ARAKAWA, Masahiko[3]

[1]Organization of Advanced Science and Technology, Kobe University, [2]Faculty of Science, Kobe University, [3]Graduate School of Science, Kobe University

Introduction: Two theories are proposed for the growth mechanism of bodies with the diameter from cm to several hundreds meters (pre-planetesimals). One is that planetesimals could form by a gravitational instability in the dust layer of a protoplanetary disk. The other is that planetesimals could form by a repeating impact coagulation of dust aggregates. In this study, we focus on the latter theory. There are some problems that planetesimals could not grow because of rebound and catastrophic disruption among pre-planetesimals caused by the increase of average density. Sakamoto (2013) did free-fall impact experiments of porous snow simulating icy pre-planetesimals by using the stainless cylinder to examine the compaction conditions, and clarified the relationship between the impact stress and the final density profile and the size of compaction area. However, the impact velocities in her study were 0.7 to 3.5 m/s, relatively lower compared to the average impact speed of pre-planetesimals. In this study, we conducted impact experiments of porous materials at $>$5 m/s to examine the compaction mechanism, impact stress, and density profile.

Experimental methods: The target was high porous snow with the initial porosities of 70 and 80% and perlite particles with the density of 85 kg/m^3 simulating the icy and rocky pre-planetesimals. We did impact experiments of snow in the cold room (-10 ℃) at ILTS, Hokkaido University, and perlite at Kobe University, by using the one-stage vertical and horizontal light gas guns. The vertical gun was used for only snow targets. The target was prepared by packing ice grains or perlite particles into the acrylic tube, up to 120 mm depth, and the blue ice grains or the red perlite particles were put into the target every 20 mm from the bottom due to measure the density changing with depth. The piston was set on the target surface in the acrylic tube, and accelerated by the projectile to compress the target. The projectiles were an elastic ball with the diameter of 25 mm for horizontal gun and same ball installed on the cylindrical sabot with the diameter of 30 mm for vertical gun. The pistons were a polycarbonate, an aluminum, and a polyacetal cylinders with the diameter of 30 mm and the height of 10-30 mm to examine the effects of piston type. The impact velocities were 2-118 m/s. The impact compaction of the target was observed by a high-speed digital camera. The shutter speed was set to be 20 to 100 μs, and the frame rate was set to be 6000 to 10000 fps.

Results: First, we measured the impact stress from the motion of piston, σ_p, and compared σ_p with the strength calculated by Kinoshita method, Y. As a result, the σ_p was almost same with the Y for both perlite and snow targets.

Next, we measured the final density of target, ρ_f, and obtained the relationship between the ρ_f and the kinetic energy or the momentum of projectile. As a result, we found that the ρ_f for perlite was determined by the kinetic energy while that for snow was determined by the momentum. Furthermore, we proposed the model of ρ_f for perlite and snow by assuming these compaction mechanisms: the perlite compressed due to the fracture of perlite particles while the snow compressed due to the decrease of area among ice grains. We compared these models with our experimental results and found that they were almost consistent with each other.

Finally, we examined the relationship between the σ_p and the final density of top layer in the target, ρ_{f1}. As a result, we obtained as ρ_{f1}=3.0${\sigma_p}^{0.8}$ for perlite and ρ_{f1}=127${\sigma_p}^{0.3}$ for snow in kPa. The data for snow at σ_p $>$100 kPa was scattered because the compaction mechanism was changed at σ_p $>$100 kPa.

Keywords: pre-planetesimal, dynamic compaction, impact experiment, final density, Kinoshita strength, compression viscosity

Japan Geoscience Union Meeting 2014
(28 April - 02 May 2014 at Pacifico YOKOHAMA, Kanagawa, Japan)

PPS21-P18 Room:Poster Time:April 29 18:15-19:30

Effect of particle size distribution on thermal conductivity of powdered materials

SAKATANI, Naoya[1*] ; OGAWA, Kazunori[2] ; HONDA, Rie[3] ; ARAKAWA, Masahiko[4] ; TANAKA, Satoshi[2]

[1]The Graduate University for Advanced Studies, [2]Institute of Space and Astronautical Science, [3]Kochi University, [4]Kobe University

Understanding about heat transport mechanism of powdered materials, such as lunar surface regolith, is important issue in order to estimate planetary thermal evolution and present thermal state. Thermal conductivity of powdered materials depends on various parameters (particle size and its distribution, temperature, compressional stress, etc.). Depending on these parameters, thermal conductivity can vary by one order of magnitude. Due to insufficiency of the experimental studies, heat transfer mechanism is not understood enough, and it is difficult to constrain in-situ thermal conductivity on planetary surface.

Our purpose is to understand the heat transfer mechanism of powdered materials under vacuum conditions by means of systematic survey of parameter dependences of the thermal conductivity. This will enable us to model the thermal conductivity, which can apply the estimation of thermal conductivity structure on planetary surface. Most of previous studies focus on the powdered samples with uniform particle size. However, actual planetary regolith has wide range of particle size from sub-μm to mm. Moreover, parent bodies of chondritic meteorites would be composed of mixture of meteoritic matrix and chondrule. In this presentation, we will report the effect of particle size distribution on the thermal conductivity under vacuum.

Glass beads mixtures of 100 μm and 200 μm in diameters were used. Prepared samples had volume mixing ratio of 1:0, 2:1, 1:1, 1:2, and 0:1. Porosity of each sample was 0.38, 0.35, 0.32, 0.35, and 0.38, respectively. The thermal conductivity of these samples was measured by line heat source method.

As a result, 100 and 200 μm glass beads of uniform sizes had 0.0023 and 0.0035 W/mK, respectively. This difference in the conductivity would be caused by the difference of radiative heat transfer. On the other hand, mixing samples had thermal conductivity of 0.0039, 0.0029, and 0.0039 W/mK for mixing ratio of 2:1, 1:1, and 1:2, respectively. These conductivities related well to porosity. There were no linear relation between thermal conductivity and mixing ratio. We found M-shaped correlation between them.

The measured thermal conductivity can be represented by the sum of solid conductivity, which is conductive contribution through contact area between the particles, and radiative conductivity, which is radiative contribution through the pore between the particle surfaces. Our results will be explained by the variation of these conductivities with particle size distribution. Therefore, it is necessary to separate the measured values into solid and radiative conductivities for explanation of our experimental results. This can be accomplished by investigation of temperature dependence of the conductivity. In this presentation, we will report dependence of solid and radiative conductivities on the particle size distribution.

Japan Geoscience Union Meeting 2014
(28 April - 02 May 2014 at Pacifico YOKOHAMA, Kanagawa, Japan)

PPS21-P19 Room:Poster Time:April 29 18:15-19:30

Measurement experiments of thermal conductivity and sound velocity in sintered glass beads

TSUDA, Shoko[1] ; OGAWA, Kazunori[1*] ; SAKATANI, Naoya[2] ; ARAKAWA, Masahiko[3] ; YASUI, Minami[3]

[1]The University of Tokyo, [2]The Graduate University for Advanced Studies, [3]Kobe University

The thermal conductivity and sound velocity of sintered particle materials (glass beads) were experimentally measured, and a correlation between them was investigated. Particles have often played important roles in the solar system history. Especially dust particles condensed in the early solar nebula formed planetesimals, and they remained as the main structure material of the bodies. The particles were then gradually sintered as temperature increased by disintegrations of radioactive isotopes. Finally, a part of planetesimals might be completely sintered and began to melt. Currently the sintered materials may also exist on the lunar and asteroid subsurface for example. Mechanical and thermal properties of such sintered materials are essential information for investigating the history of these bodies.

In the thermal issues, particles are known as a strong thermal insulator in vacuum. Although the thermal conductivity of sintered materials has never been measured, it is considered to be a value between the unsintered and a continuous rock, depending on degree of the sintering process. Concerning the sound velocity, characteristic feature depending on the sintering degree is expected to be similar to the thermal conductivity, because basically the phonon conduction is a common mechanism for both the thermal and sound phenomena in electrical insulation materials.

In this presentation, we report results of the first experiments of the thermal conductivity and sound velocity measurements in sintered particle materials. For measurement samples, 9 different blocks of sintered soda-lime glass beads were prepared: three bead diameters of 180-255, 355-500, and 710-1000 μm, and three degrees of sintering that have nearly the same porosity 40%. The cross section of sintering contact sites (neck) was evaluated for each sample. The thermal conductivity was measured by the line heat source method by a line heater and temperature sensors given in the sample in advance. The sound velocity was directly measured by a transmitter and receiver put at both ends of the block samples.

As results of the experiments, both the thermal conductivity and the sound velocity had an apparent correlation with each other, and with degree of sintering. They appeared almost in proportion to the neck diameter, which feature obviously indicates that the neck or contact size controls the bulk thermal and sound conductions, in weakly-sintered particle systems at least. These results can be directly applied to estimation of thermal and mechanical property of the ancient planetesimals. These results also suggest that the thermal conductivity of sintered materials, and also of unsintered particles probably, can be evaluated by measurements of the sound velocity.

Keywords: Particle material, Regolith, Thermal Conductivity, Sound velocity, Glass beads

Japan Geoscience Union Meeting 2014
(28 April - 02 May 2014 at Pacifico YOKOHAMA, Kanagawa, Japan)

PPS21-P20 Room:Poster Time:April 29 18:15-19:30

Experiment to know the power to pull mutually between things that are axisymmetric for the Saturn's-like magnetic axis

MASE, Hirofumi[1*]

[1]none

The magnetic axis of magnetic field in the Saturn is corresponding to the rotation axis(1). And, Saturn's rings revolve on the equatorial plane of the Saturn(2). I want to think that the reason why beautiful rings exist miraculously is related to these miraculous features. The power to pull against each other between things that are axisymmetric for the magnetic axis is generated on the plane that passes center of the axial dipole field and intersects vertically for the magnetic axis. Because the material that composes the ring is tied to the material on the 180-degree other side by the surcharge-gravitation, Saturn's rings are generated and maintained. I am making the experiment that proves the truth of this hypothesis. I introduce the result of it.

∗∗∗∗Composition of experiment (Please refer to the drawing)∗∗

"A","C":the one(34L∗25W∗25H) that natural whetstone(sandstone) was cut

"B":the one(40L∗40W∗40-80H) that 4-8 pieces of permanent magnet(anisotropic ferrite,40L∗40W∗10H,B=79mT,F=2.746kgf)s were piled up

Device box:I used "two step box" on the market and remodeled it. The front side of the left cell of this box is glazed. The front side of the right cell of this box is opening. Plywood in which "B" is set is put on the medium plate of this box to close the hole in the plate. The left cell is airtight exclusive of the top of the vinyl chloride pipe. "A" is hung from the ceiling by two strings(1,700L) and can swing freely in the left cell. The space of "B" and "A" in geostationary point is about 20mm. "C" is hung from the top board in the right cell by the string. The edge of another string is bonded on the right side of "C". (State:"C1")"C" can be separated from "B" by pulling this string from the right side of this box. (State:"C2")"C" can approach "B" by loosening this string.

∗∗∗∗Condition of experiment∗∗I experimented on the following three kinds of by changing the composition and direction of "B". Condition 1:pile 8 pieces vertically(magnetic axis is perpendicular) Condition 2:pile 4 pieces vertically(axis, perpendicular) Condition 3:pile 4 pieces horizontally(axis, horizontal right and left)

∗∗∗∗Procedure of one experiment∗∗1.I wait as much as possible until the swing of "A" stops(now"C1"). 2.I begin taking a picture of the animation of "A" with the video camera(now"C1"). 3.After 2 minutes pass, I change State from "C1" into "C2"(now"C2"). 4.After 4 minutes pass, from "C2" into "C1"(now"C1"). 5.After 6 minutes pass, from "C1" into "C2"(now"C2"). 6.After 8 minutes pass, I end taking a picture.

∗∗∗∗Result of experiment∗∗"A" swung faintly when taking a picture was begun. 1.In case of Condition 1 and 2, the swing was controlled at time zone in State "C2" of the first times, and was amplified at time zone in State "C2" of the second times. 2.In case of Condition 3, I could not confirm special change of "A" during all time.

∗∗∗∗Consideration∗∗I seem I can conclude that static electricity and magnetism don't influence the result by the comparison between Condition 2 and 3. There is a possibility that the power that I had expected was detected.

Reference literature

(1)Hori/"The School of the Universe (13th)"/NAOJ
http://th.nao.ac.jp/MEMBER/hori/pdf/HORI_2013Mar26_part1.pdf P23
(2)Hiratsuka City Museum http://www.hirahaku.jp/hakubutsukan_archive/tenmon/00000050/59.html

PPS21-P20 Room:Poster Time:April 29 18:15-19:30

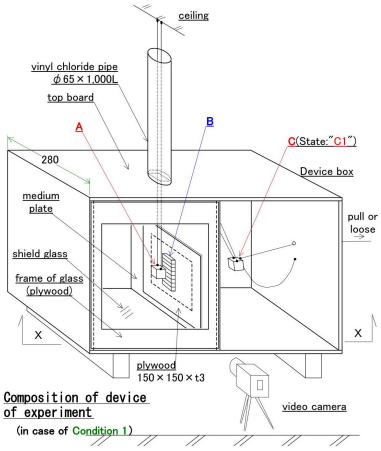

Composition of device of experiment
(in case of Condition 1)

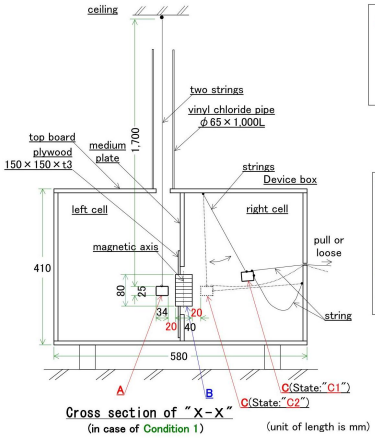

Cross section of "X-X"
(in case of Condition 1)
(unit of length is mm)

A, C : natural whetstone(sandstone)
34L × 25W × 25H

B : permanent magnet(anisotropic ferrite,40L × 40W × 10H, B=79mT,F=2.746kgf) piled up 4～8 pieces
40L × 40W × 40～80H